

Submitted to Journal of Chemical Physics

UCRL-19109 Rev.  
Preprint

c.2

RECEIVED  
JULY 1971  
RADIATION LABORATORY

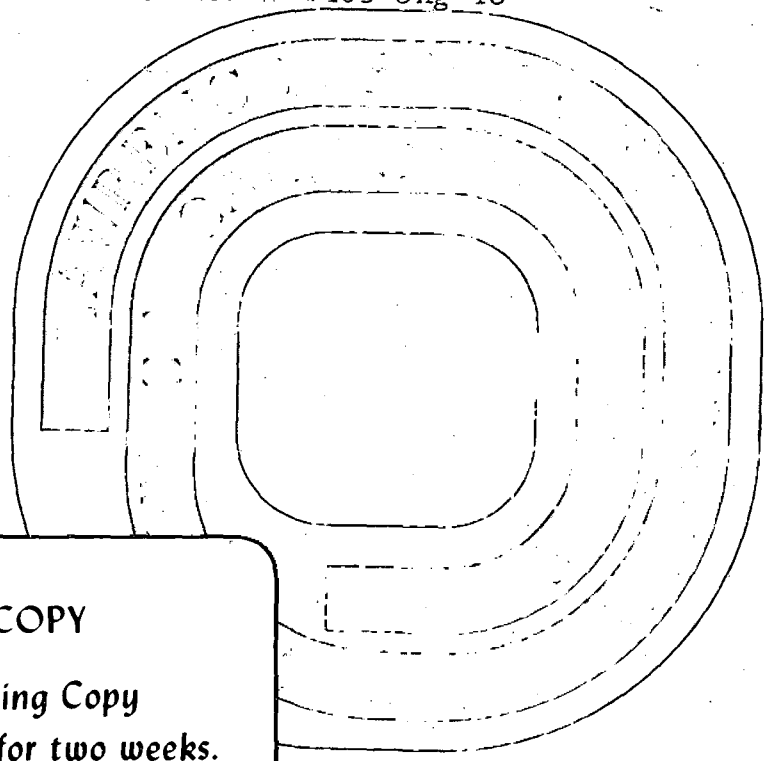
UCRL-19109 Rev. 7/71

SPECTRA AND KINETICS OF THE HYDROPEROXYL  
FREE RADICAL IN THE GAS PHASE

Thomas T. Paukert and Harold S. Johnston

July 1971

AEC Contract No. W-7405-eng-48



**TWO-WEEK LOAN COPY**

This is a Library Circulating Copy  
which may be borrowed for two weeks.  
For a personal retention copy, call  
Tech. Info. Division, Ext. 5545

UCRL-19109 Rev.

c.2

## DISCLAIMER

This document was prepared as an account of work sponsored by the United States Government. While this document is believed to contain correct information, neither the United States Government nor any agency thereof, nor the Regents of the University of California, nor any of their employees, makes any warranty, express or implied, or assumes any legal responsibility for the accuracy, completeness, or usefulness of any information, apparatus, product, or process disclosed, or represents that its use would not infringe privately owned rights. Reference herein to any specific commercial product, process, or service by its trade name, trademark, manufacturer, or otherwise, does not necessarily constitute or imply its endorsement, recommendation, or favoring by the United States Government or any agency thereof, or the Regents of the University of California. The views and opinions of authors expressed herein do not necessarily state or reflect those of the United States Government or any agency thereof or the Regents of the University of California.

SPECTRA AND KINETICS OF THE HYDROPEROXYL FREE RADICAL  
IN THE GAS PHASE<sup>1</sup>

Thomas T. Paukert and Harold S. Johnston

Department of Chemistry and Inorganic Materials  
Research Division, University of California  
Berkeley, California

ABSTRACT

The absorption spectrum of the hydrogen radical ( $\text{HO}_2$ ) has been obtained by the molecular-modulation technique. The radical was formed by the photolysis of hydrogen peroxide at 2537 Å, by the photolysis of ozone in the presence of hydrogen peroxide at 2537 Å, and by the photolysis of  $\text{Cl}_2$  in the presence of hydrogen peroxide at 3500 Å. The vibrational frequencies of  $\text{HO}_2$  have been observed to be 1095, 1390, and 3410  $\text{cm}^{-1}$ . Details of the vibrational spectrum are consistent with the molecular geometry: H-O bond distance 0.96 Å, O-O bond distance 1.3 Å, and H-O-O angle approximately 108°. The absorption spectrum of  $\text{HO}_2$  in the ultraviolet has a maximum at 2100 Å.

Kinetic analysis of the modulated absorption signals shows that the  $\text{HO}_2$  radical decays by a process second order in  $\text{HO}_2$  concentration. The rate constant for the disproportionation reaction  $\text{HO}_2 + \text{HO}_2 \rightarrow \text{H}_2\text{O}_2 + \text{O}_2$  was found to be  $3.6 \pm 0.5 \times 10^{-12} \text{ cm}^3/\text{mole} \cdot \text{sec}$  in agreement with a reported value of  $3 \times 10^{-12} \text{ cm}^3/\text{mole} \cdot \text{sec}$ .

The absorption cross section of  $\text{HO}_2$  at 1420  $\text{cm}^{-1}$ , the absorption maximum of the 1395  $\text{cm}^{-1}$  band is approximately  $5 \times 10^{-20} \text{ cm}^2/\text{molecule}$ . The absorption cross section at 2100 Å is  $4.5 \times 10^{-18} \text{ cm}^2/\text{molecule}$ .

## I. INTRODUCTION

The direct observation of free radical intermediates is an essential step in determining the mechanism of some complex chemical reactions.<sup>2</sup> Successful techniques for direct observation of free radicals include flash photolysis<sup>3,4</sup>, matrix isolation<sup>5,6</sup>, and electron spin resonance. A method that operates with low light intensities and that gives both spectra and kinetics (analogous to flash photolysis) has been developed in this laboratory.<sup>7-10</sup> The observation of the hydroperoxyl radical (HOO) by this "molecular modulation" method is the subject of this paper.

A. Indirect Evidence of HOO

The occurrence of HOO as an intermediate has been postulated in kinetic studies of the hydrogen-oxygen reactions,<sup>11-17</sup> in photochemical studies of ozone in the presence of water<sup>19-22</sup> or in the presence of hydrogen peroxide,<sup>23</sup> and in the photolysis of hydrogen peroxide.<sup>24</sup> In a study of the flash photolysis of hydrogen peroxide with direct observation of the hydroxyl radical, Greiner<sup>25</sup> showed that hydroxyl is formed directly by photolysis



and that it decays by a process first order in HO and first order in  $\text{H}_2\text{O}_2$ , presumably



Greiner searched for an absorption by HOO in the region 2500 - 10,000 Å but found nothing. The overall kinetics of the photolysis of hydrogen peroxide indicates the following reaction as the radical terminating step



B. Direct Evidence of HOO

Direct observation of  $\text{HO}_2$  was first accomplished by Foner and Hudson<sup>26</sup> who succeeded in producing hydroperoxyl radicals by the reaction



and detecting them by mass spectrometry. This radical has also been observed mass spectrometrically by Robertson<sup>27</sup> who

added  $O_2$  to a stream of H atoms, Ingold and Bryce<sup>28</sup> who reacted  $O_2$  with H atoms and with methyl radicals, and Fabian and Bryce<sup>29</sup> who studied the reaction of methane with oxygen molecules. Foner and Hudson<sup>26</sup> have reported observing the mass spectrum of  $HO_2$  formed in six different ways: the reactions of H atoms with  $O_2$  and  $H_2O_2$ , of O atoms with  $H_2O_2$ , of OH radicals with  $H_2O_2$ , the photolysis of  $H_2O_2$ , and a low-power electrical discharge of  $H_2O_2$ .

Spectroscopic detection of  $HO_2$  has been achieved by Milligan and Jacox<sup>30</sup> using the matrix isolation technique. They photolyzed an HI- $O_2$  mixture in an argon matrix at 4°K and obtained infrared absorption peaks in the regions 1040 - 1101  $cm^{-1}$ , 1380 - 1390  $cm^{-1}$ , and at 3402 and 3414  $cm^{-1}$ . These absorptions were attributed to the O-O stretching, HOO bending, and H-O stretching vibrations, respectively. The spectrum has been confirmed by Ogilvie<sup>31</sup> in an argon-neon matrix at 4°K, but his low frequency assignments are reversed.

The transient ultraviolet absorption spectrum of  $HO_2$  has been observed following the pulsed electron irradiation of oxygenated aqueous solutions by Czapski and Dorfman.<sup>32</sup> The spectrum of the radical in solution begins at approximately 3000 Å and has a maximum at 2300 Å with a molar extinction coefficient  $\alpha = 1150 M^{-1} cm^{-1}$ . Subsequent experiments in pulse radiolysis and flash photolysis of aqueous solutions have confirmed the u.v. spectra.<sup>32</sup>

Simultaneously with this work,<sup>1</sup> Troe<sup>33</sup> observed the ultraviolet spectrum of gaseous HOO between 2100 and 2800Å

at 1100°K in the thermal decomposition of hydrogen peroxide in a shock tube.

Only one <sup>direct</sup> measurement of the HO<sub>2</sub>-HO<sub>2</sub> disproportionation rate constant in the gas phase has been reported. Foner and Hudson<sup>34</sup> found a rate constant of  $3 \times 10^{-12} \text{ cm}^3/\text{molecule}\cdot\text{sec}$ . An indirect estimate of the rate constant by Burgess and Robb is a factor of 100 larger while the upper limit derived by Lewis and von Elbe from combustion studies is a factor of  $10^5$  smaller.

### C. Structure of HOO

Very little is known of the structure of the hydroperoxyl radical. Several theoretical studies of this molecule have been made, but there is no agreement. Green and Linnett<sup>35</sup> predict a bond angle between 55 and 70°; Boyd<sup>36</sup> carried out theoretical calculations which give a bond angle of 47° with the H atom at the apex of an isosceles triangle. In contrast, Walsh<sup>37</sup> predicts that the bond of HO<sub>2</sub> should lie between 90 and 180° and should be slightly less than the bond angle of HNO. The bond angle of HNO in the ground state has been found to be 108.5°. <sup>38</sup> Milligan and Jacox's<sup>30</sup> spectral work demonstrates that the O atoms of HO<sub>2</sub> are not equivalent which rules out an isosceles triangular structure. On the basis of Walsh's theory, which successfully predicts the structure of HCO and HNO, the HO<sub>2</sub> molecule is probably nonlinear with a bond angle of about 108°.

## II. EXPERIMENTAL

### A. Methods<sup>7-10</sup>

The detection and study of free radical intermediates in photochemical reactions at ordinary (moderate) light intensities present several problems. Radical concentrations are very small, on the order of  $10^{10}$  to  $10^{13}$  molecules/cm<sup>3</sup>. Spectroscopic signals are likewise very small, so small in fact, that the noise inherent in photo-detectors is many times larger than the signals themselves. Second the reactants and products are in much greater concentrations than the radicals, typically by a factor of  $10^3$  to  $10^4$ . In conventional spectroscopy any spectral overlap of reactant or product on a radical band would swamp the radical signal. The molecular modulation technique was devised to cope with these problems and, at the same time, provide information about radical reaction rates.

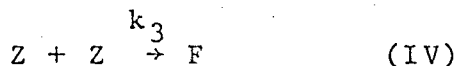
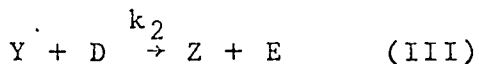
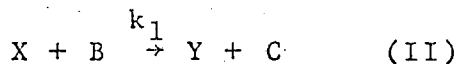
The technique is, in concept, similar to the phase-shift method of obtaining fluorescence life-times. A photolytic lamp is turned on and off so that the lamp output is a square wave. The frequency of the square wave is chosen to permit the radical concentration to reach approximately a steady value while the lamp is on and to decay to a near-zero value while the lamp is off. Thus the radical concentration and spectroscopic signal are given in A.C. component which can be extracted from the noise by using lock-in amplifiers with long time-constants. The flashing lamp also gives A.C. components to reactant and product concentrations. These components are generally less than one percent

of the total concentration, mitigating to some extent the effect of spectral overlap. A flow system is used to make the periodic variations in reactant and product concentrations oscillate about stable D.C. levels.

The various species in a photo-chemical reaction not only have components at the frequency of the flashing lamp; they also have a rich harmonic content (see below). The harmonics which determine the wave shape (square, triangular, saw-tooth, etc.) are functions of the chemical kinetics. For example, a "first-order" radical, which decays by a process first order in the concentration of that radical, has no harmonics not present in the lamp flash. On the other hand, a "second-order" radical, which decays by a process second order in the radical concentration, has even harmonics not present in the lamp flash. A lock-in amplifier tuned to the frequency of the flashing lamp extracts the fundamental frequency, a fraction of the odd harmonics, and rejects all of the even harmonics. Since the phase shift of the fundamental frequency is a strong function of chemical species and radical life-time, the necessary kinetic information can be obtained from just the fundamental frequency.

#### B. Mathematical Basis for the Method

The reaction scheme below illustrates the important types of chemical species in a modulation experiment. The species A through F are stable molecules; and X, Y, and Z are free radicals. The modulation of each species is a function of the type of species and of the elementary reaction rates.



Since the concentrations of the species in the chemical system vary periodically in time, they can be represented by a Fourier expansion of the form

$$f(\omega t) = \sum_n \left[ a_n \sin(n\omega t) + b_n \cos(n\omega t) \right] + b_0$$

where  $\omega$  is the fundamental angular frequency of the wave obtained from the period  $T$  by the relation  $\omega = 2\pi/T$ . An alternative form of the Fourier expansion is:

$$f(\omega t) = \sum_n c_n \sin(n\omega t + \delta_n) + c_0.$$

The two are related by:

$$c_n = (a_n^2 + b_n^2)^{1/2} \quad \text{and} \quad \delta_n = \tan^{-1}(b_n/a_n).$$

The coefficients  $c_n$  are amplitudes; the quantities  $\delta_n$  are phase shifts. In the following analysis, the photolytic lamp is represented by an expansion involving sine terms only, i.e., all  $b_n = 0$ . Hence all  $\delta_n = 0$ . For any chemical species, then,  $\delta_n$  is its phase shift relative to the photolytic lamp.

### 1. Reactant Decomposed by Light

The differential equation for A is:

$$\frac{d[A]}{dt} = \frac{f'}{V} [A]_0 - \sigma [A] \frac{I_0}{2} + \frac{2I_0}{\pi} \sum_{n, \text{odd}} \frac{1}{n} \sin(n\omega t) - \frac{f'}{V} [A] \quad (5)$$

where  $f'$  is the flow rate into and out of the cell in liters/sec.

V is the volume of the cell in liters

$[A]_0$  is the concentration of A entering the cell in molecules/cm<sup>3</sup>

$I_0$  is the photon flux in photons/cm<sup>2</sup>·sec

$\sigma$  is the absorption cross-section of the reactant in cm<sup>2</sup>/molecule

$[A]$  is the concentration of A

$\omega$  is the flashing frequency in radians/sec

t is the time in sec

Since  $\omega = 2\pi/T = 2\pi f$  where f is the flashing frequency in cycles/sec., we can write  $\theta = \omega t = 2\pi f t$  from which we get  $d\theta/dt = 2\pi f$  or  $dt = d\theta/2\pi f$ , giving

$$\frac{d[A]}{d\theta} = \frac{1}{2\pi f} \left( \frac{f'}{V} [A]_0 - \sigma [A] \frac{I_0}{2} + \frac{2I_0}{\pi} \sum_{n, \text{odd}} \frac{1}{n} \sin(n\theta) - \frac{f'}{V} [A] \right) \quad (6)$$

When the change in concentration over a flashing period is small compared to the total concentration ( $\Delta[A] < 10^{-2} [A]$ ),  $[A]$  on the right side of the differential equation may be regarded as a constant. Collecting the D.C. terms we have

$$\frac{d[A]}{d\theta} = \frac{1}{2\pi f} \left( \frac{f'}{V} [A]_0 - \left( \frac{\sigma I_0}{2} + \frac{f'}{V} \right) [A] - \frac{2\sigma I_0 [A]}{\pi} \sum_{n, \text{odd}} \frac{1}{n} \sin(n\theta) \right).$$

The requirement of a stable D.C. concentration means

$$\frac{f'}{V} [A]_0 - \left( \frac{\sigma I_0}{2} + \frac{f'}{V} \right) [A] = 0$$

which gives the following simplified differential equation

$$\frac{d[A]}{d\theta} = - \frac{2\sigma I_0 [A]}{2\pi^2 f} \sum_{n, \text{odd}} \frac{1}{n} \sin(n\theta).$$

As long as the concentration modulation,  $\Delta[A]$ , is much smaller than the total concentration,  $[A]$ , the equation is linear and is easily integrated<sup>39</sup> giving the concentration modulation

$$[A]_{\text{mod}} = \frac{\sigma I_o [A]}{\pi^2 f} \sum_{n, \text{odd}} \frac{1}{n^2} \cos(n\theta). \quad (7)$$

From the definition of phase shift, we see that the reactant concentration modulation has a phase shift of  $+90^\circ$  with respect to the flashing lamp. The modulation of A is seen to be a triangular wave whose amplitude is inversely proportional to the flashing frequency.

2. Radical Formed by the Initial Photo-dissociative Step and Decaying by a Process First-order in Radical Concentration

The differential equation describing the radical concentration  $[X]$  in terms of the previously defined quantities  $\sigma, [A], \omega$ , and  $I_o$  and the concentration of reactant B, is:

$$\frac{d[X]}{dt} = 2\sigma[A] \left( \frac{I_o}{2} + \frac{2I_o}{\pi} \sum_{n, \text{odd}} \frac{1}{n} \sin(n\omega t) \right) - k_1[B][X]. \quad (8)$$

This can be solved in a straight forward manner like the previous case to yield:

$$[X] = \frac{2\sigma I_o [A]}{\pi^2 f} \sum_{n, \text{odd}} \left( \frac{k_1[B]}{2\pi f} \frac{1}{n} \sin(n\theta) - \cos(n\theta) \right) / \left( \left( \frac{k_1}{2} \frac{[B]}{\pi f} \right)^2 + n^2 \right) + \frac{\sigma I_o [A]}{k_1 [B]}. \quad (9)$$

When this equation for  $[X]$ , the radical concentration, is taken to its low frequency limit we get:

$$\lim_{f \rightarrow 0} [X] = \frac{4\sigma I_o [A]}{\pi k_1 [B]} \sum_{n, \text{odd}} \frac{1}{n} \sin(n\theta) + \frac{\sigma I_o [A]}{k_1 [B]}. \quad (10)$$

This is the equation of a square wave with an amplitude of  $\sigma I_o [A]/k_1 [B]$  oscillating about a D.C. level of  $I_o [A]/k_1 [B]$ .

Thus the radical concentration has a maximum of  $2\sigma I_o [A]/k_1 [B]$ -- the radical concentration one obtains from the "steady-state" approximation for [X]. Note also that the phase shift of the radical concentration is  $0^\circ$ . At high frequencies we have:

$$\lim_{f \rightarrow \infty} [X] = \frac{2\sigma I_o [A]}{\pi^2 f} \sum_{n, \text{odd}} \frac{1}{n} \cos(n\theta) + \frac{\sigma I_o [A]}{k_1 [B]} \quad (11)$$

So [X] becomes a triangular wave with vanishing amplitude oscillating about a D.C. level equal to one-half the "steady-state" concentration. The phase shift is  $-90^\circ$ .

It is convenient to define the "life-time" of the radical, X, to be

$$\tau_1 = \frac{1}{k_1 B}$$

which is the time required for the concentration to drop by a factor of e. The behavior of the fundamental of [X] at intermediate flashing frequencies is plotted in Figure 1 as a function of the ratio of the flashing period ( $T=1/f$ ) to the radical life-time.

The phase shift of the fundamental of [X] is given by:

$$\delta = \tan^{-1}(b_1/a_1) = \tan^{-1}(-1/(k_1 [B]/2\pi f)).$$

So

$$k_1 [B] = \frac{-2\pi f}{\tan \delta}.$$

Thus the radical life-time can be found from just one phase shift measurement at one frequency if the radical species is known to be formed in the initial step and to decay by a process first-order in radical concentration.

3. Radical Formed by a Radical-Molecule Reaction and Decaying by a Process First-Order in Radical Concentration

When a radical is formed by the reaction of a preceding radical, X, with a molecule, B, and is destroyed by reaction with another molecule, D, the differential equation describing the concentration of the new radical, Y, is:

$$\frac{d[Y]}{dt} = k_1[B][X] - k_2[D][Y]. \quad (12)$$

Integration of this equation after changing the variable from t to  $\theta$  and substituting Eq. (9) for [X] gives

$$[Y] = \frac{\sigma I_o [A]}{k_2 [D]} + \frac{2\sigma I_o [A] k_1 [B]}{\pi^2 f} \sum_{n, \text{ odd}} \left( \frac{k_1 [B] k_2 [D] - (2\pi f n)^2}{(2\pi f)^2 n^2 ((k_1 [B]/2\pi f)^2 + n^2)} \sin(n\theta) - \frac{k_2 [D] + k_1 [B]}{2\pi f ((k_1 [B]/2\pi f)^2 + n^2)} \cos(n\theta) \right) / ((k_2 [D]/2\pi f)^2 + n^2). \quad (13)$$

Since the coefficients  $b_n$  are always negative and the coefficients  $a_n$  may be either positive or negative depending on the sign of  $k_1[B]k_2[D] - (2\pi f n)^2$ , the phase shift of the fundamental of [Y] may lie anywhere between  $0^\circ$  and  $-180^\circ$ . The dependence of the concentration modulation of Y on flashing frequency is determined by  $k_1[B]$ ,  $k_2[D]$ , and f. A convenient way of looking at the modulation of Y is to plot the amplitude and phase shift of the

fundamental as a function of  $T/\tau_1$  for several values of  $\tau_2/\tau_1$ . This is done in Figure 2a and b. When  $\tau_2/\tau_1$  is large, at frequencies where the primary radical X has a phase shift close to  $0^\circ$ , the secondary radical Y behaves like a primary radical. Under such conditions the life-time of Y can be easily obtained. When  $\tau_2/\tau_1$  is small, however, determination of the life-time will be difficult because the phase shift of the secondary radical Y is determined, for the most part, by the phase shift of the preceding radical. At flashing frequencies high enough to impart a substantial phase shift to the secondary radical due to its own inherent life-time, the modulation amplitude of the preceding radical is very low. As a result, the modulation amplitude of the secondary radical is also very small making detection difficult.

4. Radical Which Decays by a Process Second-Order in Radical Concentration

The differential equation for the second-order radical Z is

$$\frac{d[Z]}{dt} = k_2[D][Y] - 2k_3[Z]^2. \quad (14)$$

This equation is intractable because the equation is non-linear, and [Y] and [Z] are both functions of t. A special case of (14) is of considerable interest

$$\frac{d[Z]}{dt} = P - Q[Z]^2 \quad (15)$$

where P and Q are constant. This case can arise from (14) if the radical Y is very fast and is in phase with the exciting light. Another case occurs when the radical Z is formed directly from the primary photolysis of the reactant. A numerical solution to (14) can be readily obtained if the equation is written in two parts, one corresponding to the lamp on and one to the lamp off.

$$\frac{d[Z]}{d\theta} = \frac{1}{2\pi f} (P - Q[Z]^2) \quad -\pi \leq \theta \leq 0 \quad (16)$$

$$\frac{d[Z]}{d\theta} = -\frac{1}{2\pi f} Q[Z]^2 \quad 0 \leq \theta \leq \pi \quad (17)$$

Each of these equations can be integrated; the solution with the lamp on is

$$[Z]_{\theta} = \left(\frac{P}{Q}\right)^{\frac{1}{2}} \tanh \frac{(\theta+\pi)(PQ)^{\frac{1}{2}}}{2\pi f} \tan^{-1} \frac{[Z]_{-\pi}}{(P/Q)^{\frac{1}{2}}}$$

and with the lamp off it is

$$[Z]_{\theta} = \frac{2\pi f [Z]_0}{2\pi f + Q\theta [Z]_0}$$

Using these two equations, we may assume an initial value for  $[Z]_{-\pi}$ , calculate  $[Z]_0$  and  $[Z]_{\pi}$ , set  $[Z]_{-\pi} = [Z]_{\pi}$ , and recalculate  $[Z]_0$  and  $[Z]_{\pi}$  until  $[Z]_{\pi} = [Z]_{-\pi}$  within a desired degree of accuracy. Having found  $[Z]_{-\pi}$ , we then calculate  $[Z]$  for small increments of  $\theta$  (e.g.,  $\Delta\theta = 2\pi/100$ ). The resulting table of  $[Z]_{\theta}$  vs.  $\theta$  provides the basis for the Fourier analysis of  $[Z]$ . For the periodic function

$$[Z] = \sum a_n \sin(n\theta) + b_n \cos(n\theta) + b_0/2$$

the coefficients  $a_n$  and  $b_n$  can be found by the numerical integrations

$$a_n = \frac{1}{\pi} \sum_{i=1}^m [Z]_{\theta_i} \sin(n\theta_i) \Delta\theta$$

$$b_n = \frac{1}{\pi} \sum_{i=1}^m [Z]_{\theta_i} \cos(n\theta_i) \Delta\theta$$

where  $m$  is the number of increments of  $\theta$ . Such an analysis has been done over a wide range of flashing frequencies. The amplitude and phase shift behavior of the fundamental as a function of the ratio of flashing period to radical life-time is shown in Figure 3. Because the life-time of a second-order species depends on concentration, we define "the radical life-time" to be the half-life of the radical from its steady-state concentration. The steady-state concentration of the radical  $Z$  is

$$[Z]_{ss} = \left( \frac{2\sigma I_o [A]}{2k_3} \right)^{\frac{1}{2}} = (P/Q)^{\frac{1}{2}} \quad (18)$$

and the life-time becomes

$$\tau = \frac{1}{2k_3 [Z]_{ss}} = (PQ)^{-\frac{1}{2}} \quad (19)$$

Comparison of the life-time formulae for the first- and second-order radicals indicated how these kinetically different radicals can be distinguished experimentally. The life-time of a first-order radical, given by

$$\tau = 1/k_1 [B], \quad (20)$$

is independent of radical formation rate and inversely proportional to the concentration of a reactant involved

in the radical's decay. The life-time of a second-order radical given by (19) is inversely proportional to the square-root of the radical formation rate. Changes in reactant concentration affect the life-time only by affecting the radical formation rate. Thus varying reactant concentrations and the photolytic light intensity can provide the information necessary to determine whether the radical decay reaction is first or second order in radical concentration.

#### 5. Product of Radical Reactions

The differential equations describing the behavior of the products, C, E, and F all have the same general form:

$$\frac{dJ}{d\theta} = \frac{k'}{2\pi f} (G + H \sum \alpha_n \sin(n\theta) + \beta_n \cos(n\theta)) - \frac{f'}{V} J \quad (21)$$

where  $J = [C], [E],$  or  $[F]$

$$k' = k_1[B], k_2[D], \text{ or } k_3$$

$G =$  the D.C. level of  $[X], [Y],$  or  $[Z]^2$

and  $H =$  the modulation amplitude of  $[X], [Y],$  or  $[Z]^2$ .

The solution to this equation is

$$J = k'G \frac{V}{f'} + \frac{k'H}{2\pi f} \sum_{n, \text{ odd}} \left\{ \left[ \left( \alpha_n \frac{f'}{2\pi f V} - n\beta_n \right) \sin(n\theta) + \left( \beta_n \frac{f'}{2\pi f V} + \alpha_n \right) \cos(n\theta) \right] / \left[ \left( \frac{f'}{2\pi f V} \right)^2 + n^2 \right] \right\}. \quad (22)$$

From this equation it is apparent that if  $f'/2\pi fV \ll 1$ , the product fundamental lags the radical fundamental by  $90^\circ$ .

Note also the inverse dependence of the product modulation

amplitude on flashing frequency. This means that a product amplitude falls off faster with increases in flashing frequency than does that for a radical. The amplitude and phase shift behavior of the product of a second-order radical is presented in Figure 4.

#### 6. Reactant Attacked by a Radical

The differential equation for a reactant B which is attacked by a radical is of the same form as the equation in Sec. 5 with two minor differences: there is a flow-in term  $(f'/V)[B]_0$  and a change in sign because molecules are being lost through reaction. The solution shows that the reactant modulation leads the radical by  $90^\circ$ . Also the reactant amplitude has the same frequency dependence as a product, i.e., it falls off faster than a radical with increases in flashing frequency.

#### C. Apparatus

Two molecular modulation spectrometers were used in this work. The spectrometer used in the ultraviolet has been described by Morris.<sup>9,10</sup> The photolysis lamps used here were

mercury resonance lamps made by General Electric, Model G64T6.

All flashing frequencies referred to in the ultraviolet work <sup>below</sup> are nominal; the true frequencies are 1.22 times the nominal frequencies.

The infrared modulation spectrometer has been described before.<sup>7,10</sup> The detectors are: mercury doped germanium cooled

for use from 800 to 3000  $\text{cm}^{-1}$  and lead sulfide operating at 193°K for use between 3000 and 4000  $\text{cm}^{-1}$ .

The reaction cell has a capacity of 270 liters. The optical path in this cell is 48 meters.

#### D. Computer Coupling

The maximum integration time of 30 sec. available from R.C. networks in the lock-in amplifiers is in many instances insufficient; for this reason the experimental apparatus was coupled to a digital computer to read and store spectral data. Spectra could be taken repetitively and added together to obtain very long averaging times. Since the spectra were recorded in digital form they were amenable to further averaging by curve smoothing.

Time independent data taken from basically continuous physical experiments are not truly independent by virtue of the continuity of the physical property being measured. This fact may be exploited to reduce noise in a spectrum further by averaging closely lying data points. The amount of noise reduction obtained depends on the averaging function employed and on the number of points included in the average.<sup>40</sup> The moving average in which all points in the average are weighted equally, is the simplest example of this kind of operation; it is also the most powerful for noise reduction.<sup>40a</sup> Its use must, however, be restricted to regions narrower than a spectral slit width to avoid loss of spectral features.

In regions of the spectrum where nine or more data points were taken per spectral slit width, no more than five points were included in the average. In regions where there were less than nine data points per slit width, the number of points in the average was restricted to three.

#### E. Chemicals and Procedure

The chemicals used in these experiments were hydrogen peroxide, ozone, and helium. The liquid hydrogen peroxide was obtained from the Becco Chemical Division of FMC Corp. in 98% purity and was used without further purification.

Ozone was produced by an electrical discharge through oxygen. The oxygen had been purified by passing over hot copper turnings to oxidize any hydrocarbon impurities; an ascarite trap removed  $\text{CO}_2$ ; and finally the oxygen was dried by a trap cooled by Dry-Ice and by a  $\text{P}_2\text{O}_5$  column. The ozone in the oxygen stream was about 1%. The separation of ozone and oxygen was accomplished by adsorption of ozone on silica gel, 6-12 mesh obtained from Matheson, Coleman and Bell. The helium carrier gas in these experiments came from Air Reduction Co. in purity exceeding 99.995%.

The reactants were carried into the cell by a stream of helium gas. Helium passed over liquid hydrogen peroxide in a saturator at a flow rate of  $8400 \text{ cm}^3/\text{min}$ . The temperature of the saturator was maintained at  $25^\circ\text{C}$ . The concentration of hydrogen peroxide was set by its vapor

pressure and the rate of decomposition in the cell and at the walls of the cell and glass lines leading to the cell.

F. Hydrogen Peroxide Concentrations During the Kinetic Experiment

The concentration of hydrogen peroxide was difficult to determine because of the high rate of decomposition of the reactant on the walls of the cell and on the sides of the exhaust tubing. Consequently, spectroscopic means were employed to determine the concentration. In the infrared cell, the concentration of hydrogen peroxide was obtained from absorbance measurements at  $3600\text{ cm}^{-1}$  and the coefficient of absorption <sup>Fig. 5</sup> reported by Giguere.<sup>42</sup> The concentration during the kinetics measurements in the I.R. cell was  $(5\pm 2) \times 10^{15}$  molecules/cc. The peroxide concentration in the u.v. cell was determined from absorbance measurements <sup>Fig. 6</sup> at  $2000\text{\AA}$  and the absorption cross-section <sup>^</sup> measured by Holt et.al.<sup>43</sup> During the experiments employing one photolysis lamp, the peroxide concentration was  $1.13 \times 10^{16}$  molecules/cc; during the two-lamp experiment it was  $8.5 \times 10^{15}$  molecules/cc.

### III. RESULTS

#### A. The Infrared Spectrum

Molecular modulation absorption spectra were recorded while an ozone-hydrogen peroxide mixture in helium was being illuminated by the photolytic lamp flashing at 1.4 Hz. The ozone concentration was about  $5 \times 10^{14}$  molecules/cc; the peroxide concentration was about  $5 \times 10^{15}$  molecules/cc. The two reactants were diluted by helium at atmospheric pressure. The spectrometer slits set to 6 mm correspond to an average resolution of  $12 \text{ cm}^{-1}$ . Figure 7 shows the modulated absorption of ozone from 1050 to  $1075 \text{ cm}^{-1}$ ; the phase shift of the ozone modulation is  $+85^\circ$ , which is in the quadrant proper to a reactant destroyed by both the photolytic light and radical attack. Absorption by a second species displays a maximum at  $1127 \text{ cm}^{-1}$ . The phase shift of the second species is  $-35^\circ$  which is proper for a radical intermediate. The breadth of the region with radical phase shift ( $1080$  to  $1140 \text{ cm}^{-1}$ ) indicates that the absorption by the second species is quite broad and may well extend below  $1080 \text{ cm}^{-1}$ , but the ozone absorption is so intense that it obscures all else.

The photolysis of ozone and hydrogen peroxide at 1.4 Hz under the same chemical conditions as above was studied in the infrared region  $1340$  to  $1500 \text{ cm}^{-1}$ . Fig. 8a  
The resolution in this region with the slits opened to six mm is  $12 \text{ cm}^{-1}$ . Another spectrum of this region, obtained under a resolution of  $8 \text{ cm}^{-1}$ , is shown in Figure 8b. Both spectra show a strong absorption

with a radical phase shift between 1350 and 1440  $\text{cm}^{-1}$ . An absorbance minimum occurs at 1390  $\text{cm}^{-1}$ . The sharp peaks at 1408 and 1425  $\text{cm}^{-1}$  in Figure 8a and at 1368, 1378, and 1425  $\text{cm}^{-1}$  in Figure 8b are narrower than the resolution of the spectrometer and cannot be regarded as spectral features. The spectrum in this region then consists of a pair of peaks centered at 1390  $\text{cm}^{-1}$  and separated by about 42  $\text{cm}^{-1}$ .

The last region in the infrared which shows modulated absorption is between 3300 and 3605  $\text{cm}^{-1}$ . This region was studied under the same chemical conditions as the previous two at a flashing frequency of 1.4 Hz. The resolution in this region varied from 18 to 25  $\text{cm}^{-1}$ , at 3300  $\text{cm}^{-1}$  to at 3600  $\text{cm}^{-1}$ . The modulated absorption spectrum shown in Figure 9 is the result of sixteen scans and a three point curve smooth. The absorption maximum at 3600  $\text{cm}^{-1}$  is very similar to the hydrogen peroxide peak in Figure 5 and has a  $+90^\circ$  phase shift due primarily to hydrogen peroxide. At lower infrared frequencies new absorption peaks are evident which cannot be assigned to either hydrogen peroxide or water because the new absorption is strongest where both water and peroxide absorption is weak, i.e., between 3350 and 3450  $\text{cm}^{-1}$ . Furthermore the phase shift of the new absorption is displaced toward the radical quadrant, but the phase shift never reaches a constant value typical of single species absorption so there must still be some peroxide component in the signal. In addition to the main peak which extends from 3380 to 3440  $\text{cm}^{-1}$ ,

there are several smaller peaks at 3550, 3505, 3470, 3345, and 3312  $\text{cm}^{-1}$ . These peaks are not present in the spectrum of water or hydrogen peroxide. The pattern of peaks does not fit the position of Q and P branch lines of the OH radical<sup>45</sup> which is known to be present in this chemical system. Later it will be shown that these peaks are consistent with the best current estimates of the structure of  $\text{HO}_2$ .

Another series of experiments was carried out photolyzing hydrogen peroxide in helium with no ozone. The hydrogen peroxide concentration during these experiments was  $5 \times 10^{15}$  molecules/ $\text{cm}^3$  in one atmosphere of helium. Signals were much weaker in the peroxide system than in the ozone and peroxide system because the absorption cross-section of hydrogen peroxide at 2537Å is about 0.01 that of ozone. The spectra obtained in the region 1000 to 1150  $\text{cm}^{-1}$  were quite noisy so six separate spectra each the result of from four to nine multiple sweeps and five-point curve smoothing are presented in Figure 10. In spite of the large amount of noise in Figure 10, certain broad features can be inferred. The observed phase shifts from 1065 to 1135  $\text{cm}^{-1}$  lie predominately in the radical quadrant. An absorption maximum occurs at approximately 1120  $\text{cm}^{-1}$  --very close to the maximum observed in the ozone-peroxide system (Figure 7). A second absorption maximum in Figure 10 appears to be at 1075  $\text{cm}^{-1}$ , with a minimum between 1090 and 1100  $\text{cm}^{-1}$ .

When the photolysis of hydrogen peroxide under the same conditions was studied in the region 1350 to 1520  $\text{cm}^{-1}$ , the spectrum presented in Figure 11 was obtained. This spectrum includes twelve scans and a five-point curve smooth. A pair of peaks separated by 45  $\text{cm}^{-1}$  and centered at 1395  $\text{cm}^{-1}$  dominates the spectrum. The phase shift of these two peaks is near  $-45^\circ$ . In another series under the same conditions, the progressive enhancement of this band by multiple-scanning and curve smoothing techniques is shown in Figure 12.

#### B. Kinetic Results

During the photolysis of hydrogen peroxide the dependence of the modulated absorption peaks at 1075, 1120, 1373, and 1420  $\text{cm}^{-1}$  on flashing frequency was studied. In these experiments the infrared spectrometer was set at a fixed I.R. frequency and the modulation signal was recorded by the computer every 10 sec for a period of ten to thirty min. The hydrogen peroxide concentration was  $5 \times 10^{15}$  molecules/ $\text{cm}^3$ . The helium carrier gas at a pressure of one atmosphere flowed through the cell at 8.4 l/min. Room temperature

during these runs was 22°C. Flashing frequency was varied from 1/4 Hz to 4 Hz.

The observed phase shifts, each the result of from ten to thirty min. of averaging, are plotted in Figure 13. The average phase shift at each flashing frequency is indicated in Figure 13 by an arrow. The solid curve in the figure is the calculated curve for a second-order radical. The position of the calculated curve on the time axis gives the quantity  $(PQ)^{1/2}$ ; it is 5.55 sec<sup>-1</sup>.

### C. The ultraviolet Spectrum

Two series of experiments were carried out in obtaining the ultraviolet spectrum of HOO between 1950 and 2500 Å. In one series H<sub>2</sub>O<sub>2</sub> in one atmosphere of He was photolyzed at 2537 Å. The mechanism is presumably reactions (1), (2), and (3). After the ultraviolet spectrum of HOO had been observed in this system, Dr. Earl Morris<sup>46</sup> checked the results in a different chemical system: the photolysis of Cl<sub>2</sub> between 3200 and 3800 Å in the presence of H<sub>2</sub>O<sub>2</sub>. The expected elementary reactions are



In a preliminary experiment, a modulation absorption spectrum was obtained from 2450 to 2000 Å during the photolysis of H<sub>2</sub>O<sub>2</sub> at 1x10<sup>16</sup> molecules/cc, at 1 Hz photolysis frequency,

in an atmosphere of helium flowing at 8.4 l/min. The modulation absorption was measured at 50 Å intervals with a spectral resolution of 13.3 Å. The spectrum showed an absorption band with a peak at 2100 Å, with phase shift between  $-15.8^\circ$  and  $-24.0^\circ$  (which is in the radical quadrant), and a variation of phase shift with wave length that suggests the presence of two modulated species. The same spectral region was examined at 1/4 Hz, and the results are shown in Figure 14. At this frequency the phase shift of the modulation displays a strong dependence on wave length, clearly indicating the presence of two species one of which is relatively more important at 1/4 Hz than at 1 Hz.

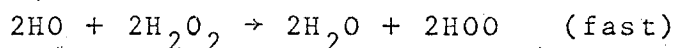
Since the phase shift at 1/4 Hz is in a reactant quadrant and since reactant amplitudes show a stronger dependence on flashing frequency than <sup>do</sup> radical amplitudes, the species gaining importance at 1/4 Hz must be the reactant hydrogen peroxide. The shape of the hydrogen peroxide absorption spectrum is well-known<sup>43,44</sup> and agrees closely with the spectrum obtained in our laboratory (Figure 6). It is evident that hydrogen peroxide could be contributing to the modulated spectrum.

#### D. Dependence of the UV Spectrum on Flashing Frequency

The response of the modulated absorption at 2200 Å to variations in flashing frequency was studied from 1/4 to 32 Hz. The conditions of the experiment were set as closely as possible to the conditions under which the spectrum (Figure 14) was

obtained; the hydrogen peroxide concentration was  $1.13 \times 10^{16}$  molecules/cm<sup>3</sup>. The phase shift is plotted against log T where T is flashing period in Figure 15; the theoretical second-order radical curve is included in the figure for comparison with the observed results. At low frequencies the observed phase shift is too positive for a pure radical signal. Apparently a reactant is becoming progressively more important as the flash period increases, agreeing with the previous results.

As has been shown before<sup>10</sup>, two modulation spectra that overlap in wave length can be resolved if the kinetic behavior (phase shift) of the two species is substantially different. The mechanism is rewritten in the following way



Three molecules of H<sub>2</sub>O<sub>2</sub> disappear with absorption of one photon, and two molecules of HOO are formed. Two molecules of HOO disappear according to reaction (3), and one molecule of H<sub>2</sub>O<sub>2</sub> is reformed. From this mechanism the differential equations are

$$\frac{d[\text{H}_2\text{O}_2]}{dt} = -3\sigma_2[\text{H}_2\text{O}_2]I + k_3[\text{HOO}]^2 \quad (25)$$

$$\frac{d[\text{HOO}]}{dt} = 2\sigma_2[\text{H}_2\text{O}_2]I - 2k_3[\text{HOO}]^2 \quad (26)$$

The steady-state relations are

$$[\text{HOO}]_{\text{ss}} = (\sigma_2 [\text{H}_2\text{O}_2] I / k_3)^{\frac{1}{2}} \quad (27)$$

$$\tau_{\text{ss}} = (4k_3 \sigma_2 [\text{H}_2\text{O}_2] I)^{-\frac{1}{2}} \quad (28)$$

The values of light intensity  $I$ , average peroxide concentration, and peroxide absorption cross section  $\sigma_2$  are known. For square wave photolysis of period  $T$ , the concentration profiles of both  $\text{H}_2\text{O}_2$  and  $\text{HOO}$  can be calculated uniquely for a given value of the ratio of period  $T$  to steady-state half-life  $\tau_{\text{ss}}$

$$\rho = T / \tau_{\text{ss}}$$

These concentration profiles were computed for a wide range of values of  $\rho$ , 0.05 to 333; and fourier analyses of the concentration profiles gave the fundamental amplitude and phase shift. At flashing frequencies of 8 Hz or greater, the reactant amplitude is so small that it may be neglected entirely; and the resulting plot of phase shift against flashing frequency (Figure 15) gives the value of  $\rho$ . With our tables of phase and amplitude as a function of  $\rho$ , the observed signal can be decomposed into radical amplitude and reactant amplitude from the observed net phase shift. This procedure is tested for the 1/4 Hz data of Figure 14, and the results are given in Figure 16. The observed resolution of amplitude from the experimental data agrees very well with the theoretical curve, which justifies the

application of this treatment of the data. With the availability of this method of resolving the overlapping spectra, an extensive set of data were taken over a wide range of wavelength and photolysis periods.

In another set of experiments, modulation spectra of the entire 2450 to 2000 Å region were obtained at flashing frequencies from 1/4 to 16 Hz. The spectra were acquired at 50 Å intervals with a resolution of 13.3 Å. The hydrogen peroxide was again carried into the reaction cell by a stream of helium flowing at 8.4 l/min. Two photolysis lamps were used. Because of the greater light intensity, the hydrogen peroxide concentration was lower than in the previous experiment. The concentration of peroxide in the two-lamp experiment was  $8.5 \times 10^{15}$  molecules/cm<sup>3</sup>. The observed spectra acquired at the various flashing frequencies in this experiment are shown in Figures 17 and 18. Each spectrum has its most negative phase shift between 2150 and 2250 Å usually at 2200 Å. The phase shift at 2200 Å is plotted against log T and the model curve is fitted to the high frequency data, i.e., 2, 4, and 8 Hz. The spectrum at 16 Hz is not used here because it is quite noisy. The 1/4 Hz spectrum is decomposed into  $-8.2^\circ$  and  $93.7^\circ$  components. The  $93.7^\circ$  component is fit by the method of least squares to the known hydrogen peroxide spectrum to obtain the amplitude of the peroxide modulation at 1/4 Hz. The phase shift and amplitude behavior of the reactant as a function of flashing frequency is known from the model, so the reactant contribution at

each flashing frequency can be calculated and subtracted from the experimental data to get the modulation signal of the radical at each flashing frequency and measured wave length.

The average phase shift of the radical over the 2000-2500Å region is plotted against log T (Figure 19).

A curve results that fits the second-order radical function within the experimental error. The position of the curve gives a value of  $(PQ)^{1/2}$  of  $14.5 \text{ sec}^{-1}$ .

#### E. The Disproportionation Rate Constant

The differential equation for HOO radical formation and second order decay may be written (compare Eq. 16)

$$\frac{dX}{dt} = P - QX^2$$

The correlation of phase shift with photolysis period (Figures 13,15,19) gives the product PQ. The difference in  $\text{H}_2\text{O}_2$  decomposition in the light and in the dark gives P.

The rate constant  $k_3$  is thus given by

$$k_3 = \frac{Q}{2} = \frac{(PQ)}{2P}$$

With respect to this rate constant, the results from the infrared (Figure 13) and ultraviolet (Figures 15 and 19) studies are summarized in Table I. The value of the rate constant is

$$k_3 = (3.6 \pm 0.5) \times 10^{-12} \text{ cc/particle-sec.}$$

where  $k_3$  is defined by

$$-\frac{d[\text{HOO}]}{dt} = 2k_3[\text{HOO}]^2$$

F. Absorption Coefficients of the Hydroperoxyl Radical

The absorption coefficient  $\sigma$  is defined by the equation  $-\Delta I/I = \sigma \Delta n l$  for small changes in the transmitted light intensity through an absorbing medium of length  $l$  caused by small changes in the concentration of the absorbers  $\Delta n$ . In our spectroscopic systems, the optical path length is known and the modulated absorbance  $\Delta I/I$  is measured. In the limit of very long photolysis periods  $T$  the radical amplitude is given by

$$\Delta n = [\text{HOO}]_{ss} = (P/Q)^{1/2}$$

The observed quantities are  $P$  and  $PQ$ . Thus

$$\Delta n = P/(PQ)^{1/2}$$

The absorbance  $\Delta I/I$  is measured at finite flashing frequencies and must be corrected to the low frequency limit. The observed phase shift and the model second-order radical curves specify the ratio of measured absorbance at each flashing frequency to the absorbance at the low frequency limit. The experiments in the ultraviolet cell provide a considerable body of data from which to calculate the cross-section for absorption. From the two-lamp experiment the spectra obtained at 1/4, 1, 2, and 4 Hz were used to determine the absorption coefficient. (The amplitude of the spectrum at 1/2 Hz is not used because it is abnormally small.) Both the spectra at 1/4 and 1 Hz obtained from one-lamp experiments were used for another determination of the absorption coefficient. The appropriate data and the results of this

calculation are given in Table II. At the absorption peak of the hydroperoxyl radical its absorption coefficient is to the base e:  $4.5 \times 10^{-18}$  cm<sup>2</sup>/molecule; to the base ten:  $2.0 \times 10^{-18}$  cm<sup>2</sup>/molecule. The absorption coefficient of this radical at its peak has been found in aqueous solution<sup>40</sup> to be (base 10):  $1.9 \times 10^{-18}$  cm<sup>2</sup>/molecule. The absorption cross section as a function of wave length between 1950 and 2450 Å is given by Figure 20.

The infrared absorption of HO<sub>2</sub> is strongest at 1420 cm<sup>-1</sup> where ΔI/I is observed to be  $1.56 \times 10^{-4}$  under conditions which give the radical a phase shift of approximately -40°. In the low frequency limit ΔI/I =  $2 \times 10^{-4}$ . The concentration modulation of HO<sub>2</sub> in the low frequency limit is

$$\begin{aligned}\Delta[\text{HO}_2] &= (\text{P/Q})^{1/2} \\ &= \left( \frac{4.5 \times 10^{12} \text{ molecules/cm}^3 \cdot \text{sec}}{7.1 \times 10^{-12} \text{ cm}^3/\text{molecules} \cdot \text{sec}} \right)^{1/2} \\ &= 8 \times 10^{11} \text{ molecules/cm}^3\end{aligned}$$

The optical path is 48 meters; the absorption coefficient to the base e is  $5 \times 10^{-20}$  cm<sup>2</sup>/molecule. Because of uncertainties in the hydrogen peroxide concentration when the spectra was obtained, this figure may be in error by as much as a factor of two.

G. HOO Spectrum in the Photolysis of Cl<sub>2</sub> in the Presence of H<sub>2</sub>O<sub>2</sub>

After the ultraviolet spectrum of HO<sub>2</sub> had been observed in the photolysis of hydrogen peroxide, Dr. Earl Morris<sup>46</sup>

conducted experiments to observe  $\text{HO}_2$  in photolysis of chlorine in the presence of hydrogen peroxide. Two G.E. F64T6-BL black lamps provide the photolysis light over the region 3200 to 3800 Å. The photon flux was  $4.2 \times 10^{16}$  photons/cm<sup>2</sup>·sec.; the effective cross-section for absorption of the photolysis light by chlorine is  $9.2 \times 10^{-20}$  cm<sup>2</sup>/molecule. The absorption cross-section of hydrogen peroxide at these wave lengths is very low ( $< 2 \times 10^{-21}$  cm<sup>2</sup>/molecule). The reactant concentrations during the photolysis were:  $[\text{Cl}_2] = 1.7 \times 10^{16}$  molecules/cm<sup>3</sup> and  $[\text{H}_2\text{O}_2] = 1.5 \times 10^{16}$  molecules/cm<sup>3</sup>. The observed modulation spectrum at 2 Hz is presented in Table III. In this system the change in  $\text{H}_2\text{O}_2$  amplitude is so small that the entire signal below 2400 Å is essentially due to  $\text{HO}_2$ . These results were normalized to the other data at the peak at 2100 Å, and the data are given in Figure 20.

## Discussion

### 1. The infrared Spectrum

The most notable difference between the infrared spectrum of  $\text{HO}_2$  in the gas phase obtained by molecular modulation and the spectrum acquired by matrix isolation is the presence of multiple peaks. The gas phase spectrum should, if the resolution is good enough, display rotation-vibration features unobtainable in the matrix.

The nature of such features is dependent on the structure of the molecule and at present the structure of  $\text{HO}_2$  is largely unknown. Walsh<sup>37</sup> has predicted that  $\text{HO}_2$  should have a bent configuration with a slightly smaller bond angle than  $\text{HNO}$  and that both molecules should have bond angles greater than  $90^\circ$ . His model for  $\text{HNO}$  was found to be correct by Dalby<sup>38</sup>, who determined the bond angle to be  $108.5^\circ$  in the ground state and  $116.2^\circ$  in the first excited state. In view of Walsh's success with  $\text{HNO}$ , it is reasonable to accept his conclusions regarding  $\text{HO}_2$ . As a lower limit on the  $\text{HO}_2$  bond angle, we may take the  $\text{H-O-O}$  angle in hydrogen peroxide which is  $94.8^\circ$ . The  $\text{HO}_2$  bond angle, then, is probably near  $108^\circ$ , but is surely within the range  $95-116^\circ$ .

The bond lengths of the hydroperoxyl radical present less of a problem. The  $\text{O-H}$  bond in the molecules  $\text{H}_2\text{O}_2$ ,  $\text{H}_2\text{O}$ , and  $\text{OH}$  is  $0.96 \pm 0.01 \text{ \AA}$ <sup>45,47,48</sup>, so a bond length of  $0.96 \text{ \AA}$  is reasonable for  $\text{HO}_2$ . The  $\text{O-O}$  bond length is less certain, but must lie between  $1.21 \text{ \AA}$ --the  $\text{O-O}$  bond distance in  $\text{O}_2$ --and  $1.45 \text{ \AA}$ --the  $\text{O-O}$

distance in  $\text{H}_2\text{O}_2$ . The O-O bond in ozone is 1.28 Å and the bond in  $\text{HO}_2$  is probably close to that, as the O-O bonds in both molecules have a bond order of 1 1/2. Boyd<sup>36</sup> used 1.3 Å in her a priori calculations on  $\text{HO}_2$ . The precise value in this case is not important, however, as the calculations show that the only rotational constant large enough to be seen in our system is relatively insensitive to the O-O bond length.

The rotational constants calculated for this model of  $\text{HO}_2$  are presented in Table IV. The molecule has one large rotational constant and two small and nearly equal ones. Thus the symmetric rotor approximation is appropriate. The allowed rotational transitions for a symmetric top are: for a parallel band  $\Delta J = 0, \pm 1$  and  $\Delta K = 0$  for  $K \neq 0$  and  $\Delta J = \pm 1$  and  $\Delta K = 0$  for  $K = 0$ ; for a perpendicular band  $\Delta J = 0, \pm 1$  and  $\Delta K = 1$ .<sup>49</sup> These selection rules give rise to the parallel and perpendicular rotation-vibration band structure of a symmetric top. If the asymmetric rotor has only a small degree of asymmetry, its rotation-vibration band structure will be a hybrid of parallel and perpendicular components.

A parallel band consists of a superposition of a number of sub-bands, one for each value of  $K$ , having P, Q, and R branches. The complete parallel band, neglecting the interaction of rotation and vibration, has a strong Q branch flanked by P and R branches similar to a diatomic molecule.

A perpendicular transition leads to a band consisting of the superposition of a number of sub-bands, one for each value

of K, having P, Q, and R branches. Because of the change in the quantum number K ( $\Delta K = \pm 1$ ), the sub-bands do not coincide so that the spectrum shows the individual Q branches on top of a diffuse unresolved background.

Since  $\text{HO}_2$  is only slightly asymmetric, we can construct a general picture of its parallel and perpendicular bands using  $A = 20 \text{ cm}^{-1}$  and  $B = 1.2 \text{ cm}^{-1}$ --the average of the two minor rotational constants. The parallel Q branches will occur at  $\nu_0$ , the vibrational frequency. The P and R branch separation found from the room temperature population distribution is  $42 \text{ cm}^{-1}$ . The perpendicular Q branches are positioned at:

$$\nu_Q = \nu_0 + (A-B) + 2(A-B)K \quad K = 0, 1, 2, \dots$$

and

$$\nu_Q = \nu_0 + (A-B) - 2(A-B)K \quad K = 1, 2, 3, \dots$$

Thus the Q branches would be positioned at:

$$\nu_0 \pm 19 \text{ cm}^{-1}$$

$$\nu_0 \pm 57 \text{ cm}^{-1}$$

$$\nu_0 \pm 95 \text{ cm}^{-1}$$

$$\nu_0 \pm 143 \text{ cm}^{-1}$$

Taking  $\nu_0$  to be  $3410 \text{ cm}^{-1}$ , the perpendicular band would have Q branches at 3429, 3467, 3505, 3553, 3391, 3353, and  $3312 \text{ cm}^{-1}$ . If the spectrum were a hybrid of the two types of bands, the parallel band with its Q branch at  $3410 \text{ cm}^{-1}$  and its P and R branches peaking at about 3431 and  $3389 \text{ cm}^{-1}$  could merge with the perpendicular Q branches at 3429 and  $3391 \text{ cm}^{-1}$  forming one broad intense peak, a likely possibility in low resolution work such as this. The observed peaks (Figure 9) at 3312, 3345, 3470, 3505, and  $3550 \text{ cm}^{-1}$  and a broad peak from 3380 to  $3440 \text{ cm}^{-1}$  fit well with the calculated peak positions.

The low frequency absorptions at  $1395\text{ cm}^{-1}$  and  $1100\text{ cm}^{-1}$  display a simpler structure. Each band has a pair of peaks separated by about  $45\text{ cm}^{-1}$ , very close to the P-R separation expected from a parallel band. Neither band gives any evidence of a Q branch. This is in accordance with the predictions of Gerhard and Dennison<sup>50</sup> who show that the intensity of the Q branch of a parallel band relative to the P and R branches becomes small as  $I_A/I_B$  is about 16.5. This leads to a ratio of Q branch intensity to P + R branch intensity of less than 0.1.

The infrared absorption frequencies observed in the gas phase are compared with the frequencies of the molecule isolated in a low temperature matrix in Table V. None of our data permits a positive assignment of the observed frequencies to vibrational modes. The assignments of Milligan and Jacox of the  $1101\text{ cm}^{-1}$  band to the 0-0 stretching vibration and their  $1389\text{ cm}^{-1}$  band to the bending vibration seem more reasonable than the reverse assignments by Ogilvie. An 0-0 stretching vibration at  $1110\text{ cm}^{-1}$ ,<sup>51</sup> and a bending vibration near  $1390\text{ cm}^{-1}$  agrees with an estimate of  $1380\text{ cm}^{-1}$  for the H-O-O symmetric bending vibration of  $\text{H}_2\text{O}_2$  by Redington et al.<sup>47</sup>

## 2. The Ultraviolet Spectrum

The ultraviolet absorption spectrum of  $\text{HO}_2$  obtained in this laboratory agrees with that observed by Troe<sup>33</sup>, except that Troe did not observe the peak at 2100 (Troe's recent studies, however, have located a maximum near 2100 Å).

and others

The spectrum reported by Czapski and Dorfman<sup>^</sup> in aqueous solution has its maximum at 2300 Å in contrast with the maximum we observe at 2100 Å. It is well known that a solvent can have a profound effect on the wave length of maximum absorption in the electronic spectra of molecules.<sup>52-58</sup> The maximum may be shifted to either higher energies (blue shift) or to lower energies (red shift) depending on the solute, solvent, and the nature of the transition involved. A red shift implies stabilization of the excited state relative to the ground state by interaction with the solvent. Conversely, a blue shift implies stabilization of the ground state relative to the excited state. Numerous workers have attempted to correlate solvent effects with the dipole moment of the solute and the dielectric constant of the solvent,<sup>52,53,57,59</sup> the refractive index of the solvent,<sup>52,53,57</sup> molar volume of the solute or solvent,<sup>53,54</sup> and hydrogen bonding between solvent and solute molecules.<sup>58</sup>

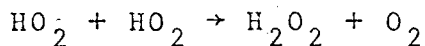
The absorption maximum in the spectrum of HO<sub>2</sub> obtained in this laboratory is separated from the maximum in aqueous solution by 4100 cm<sup>-1</sup>. The well-known correlation of a red shift in aqueous solution with molecules experiencing a  $\pi \rightarrow \pi^*$  transition and capable of forming hydrogen bonds with water can be used to explain part of the shift we have here. The transfer of electron density from central regions of the molecule in the ground state to peripheral regions in the excited state can promote the formation of a hydrogen

bond in the excited state. The magnitude of the resulting red shift depends on the strength of the hydrogen bond formed and is usually less than  $2400 \text{ cm}^{-1}$ .<sup>58</sup> The remaining part of the red shift may be due to some other interaction with the solvent or to a solvent induced change in the geometry of the  $\text{HO}_2$  molecule.

### 3. The Disproportionation Rate Constant

The determination of the  $\text{HO}_2 - \text{HO}_2$  disproportionation rate constant is based on the assumption that the reaction forming  $\text{HO}_2^-$  ( $\text{OH} + \text{H}_2\text{O}_2 \rightarrow \text{H}_2\text{O} + \text{HO}_2^-$ ), is fast, i.e., the OH concentration modulation is a square wave. The rate constant for this reaction at room temperature is  $8.15 \times 10^{-13} \text{ cm}^3/\text{molecule}\cdot\text{sec}$ .<sup>60</sup> The hydrogen peroxide concentration in our experiments was about  $1 \times 10^{16} \text{ molecules/cm}^3$ . From these two quantities we can easily calculate the time required for the OH radical to reach its "steady-state" concentration or to decay to zero. This time is approximately  $4\tau$  where  $\tau = 1/k[\text{H}_2\text{O}_2]$ . The OH life-time  $\tau$  is, then, about  $10^{-4} \text{ sec}$ , and the concentration modulation of OH is very nearly a square wave when the flashing period is greater than  $10^{-2} \text{ sec}$ . Most of our work was done at flashing periods greater than  $10^{-1} \text{ sec}$ .

The elementary rate constant for the reaction



has been found in this work to be  $k_r = 3.6 \pm .5 \times 10^{-12} \text{ cm}^3/\text{molecule}\cdot\text{sec}$ . This compares well with the value obtained by Foner and Hudson<sup>34</sup> which is  $3 \times 10^{-12} \text{ cm}^3/\text{molecule}\cdot\text{sec}$ .

REFERENCES

1. Thomas T. Paukert, Ph.D. Thesis, University of California, Berkeley (1969); Lawrence Radiation Laboratory Report UCRL-19109, November (1969). This work was supported by the Atomic Energy Commission, and in its early stages by the National Air Pollution Control Administration, U.S. Public Health Service, Grant AP-00104.
2. H.S. Johnston and F. Cramarossa, Advances in Photochemistry 4, 1. Interscience Publishers, New York (1966).
3. R.G.W. Norrish and B.A. Thrush, Quart. Rev. (London) 10, 149 (1956).
4. R.G.W. Norrish, Proc. Chem. Soc. 1958, 247; R.G.W. Norrish, Am. Sci. 50, 131 (1962); R.G.W. Norrish, Science 149, 1470 (1965); R.G.W. Norrish, Chem. Brit. 1, 289 (1965).
5. A.M. Bass and H.P. Broida (editors), Formation and Trapping of Free Radicals, Academic Press, New York (1960).
6. G. Pimentel, E. Whittle, and D.A. Dows, J. Chem. Phys. 22, 1943 (1954); G. Pimentel, V. Bondybey, and P.N. Noble, J. Chem. Phys. 55, 0000 (1971).
7. H.S. Johnston, G.E. McGraw, T.T. Paukert, L.W. Richards, and J. van den Bogaerde, Proc. Natl. Acad. Sci. 57, 1146 (1967).
8. J. van den Bogaerde, Ph.D. Thesis, University of California, Berkeley (1969).
9. E.D. Morris, Ph.D. Thesis, University of California, Berkeley (1969).
10. H.S. Johnston, E.D. Morris, Jr., and Jack Van den Bogaerde, J. Am. Chem. Soc. 91, 7712 (1969).

11. A.L. Marshall, J. Phys. Chem. 30, 34, 1078 (1926).
12. H.S. Taylor, Trans. Faraday Soc. 21, 560 (1926).
13. B. Lewis and G. von Elbe, Third Symposium on Combustion and Flames and Explosion Phenomena, Williams and Wilkins Co., Baltimore (1949) p. 484.
14. B. Lewis and G. von Elbe, Combustion, Flames, and Explosions of Gases, Academic Press, New York (1961).
15. R.R. Baldwin, L. Mayor, and P. Doran, Trans. Faraday Soc. 56, 93 (1960).
16. R.R. Baldwin and L. Mayor, Trans. Faraday Soc. 56, 80, 103 (1960).
17. R.H. Burgess and J.C. Robb, Chem. Soc. Spec. Pub. No. 9, 167 (1957).
18. G.J. Minkoff and C.F.H. Tipper, Chemistry of Combustion Reactions, Butterworths, London (1962).
19. L.J. Heidt and G.S. Forbes, J. Am. Soc. 56, 1671, 2365 (1934).
20. D.H. Volman, J. Am. Chem. Soc. 73, 1018 (1951).
21. R.G.W. Norrish and R.P. Wayne, Proc. Roy. Soc. A288, 200 (1965).
22. W.D. McGrath and R.G.W. Norrish, Proc. Roy. Soc. A254, 317 (1960).
23. D.H. Volman, Advances in Photochemistry 1, 43, Interscience Publ., New York (1963).
24. D.H. Volman, J. Chem. Phys. 17, 947 (1949).
25. N.R. Greiner, J. Chem. Phys. 45, 99 (1966); J. Phys. Chem. 72, 406 (1968).
26. S.N. Foner and R.L. Hudson, J. Chem. Phys. 36, 2681 (1962);

- S.N. Foner and R.L. Hudson, *J. Chem. Phys.* 21, 1608 (1953).
27. A.J.B. Robertson, Applied Mass Spectrometry, Institute of Petroleum, London (1954).
28. K.U. Ingold and W.A. Bryce, *J. Chem. Phys.* 24, 360 (1956).
29. D.J. Fabian and W.A. Bryce, Seventh International Symposium on Combustion, Butterworths Scientific Publications, London (1959) p. 150.
30. D.E. Milligan and M.E. Jacox, *J. Chem. Phys.* 38, 2627 (1963), 40, 605 (1964).
31. J.F. Ogilvie, *Spectrochimica Acta* 23A, 737 (1967).
32. (a) G. Czapski and L.M. Dorfman, *J. Phys. Chem.* 68, 1169 (1964); (b) H.J. Bielski and H.A. Schwarz, *J. Phys. Chem.* 72, 3836 (1968); (c) D. Behar and G. Czapski, *Israel J. Chem.* 8, 699 (1970).
33. J. Troe, *Ber. Bunsengesellschaft Phys. Chem.* 73, 946 (1969); also recent private communications.
34. S.N. Foner and R.L. Hudson, Mass Spectrometry of Inorganic Free Radicals, *Advances in Chemistry Series No. 36* (1962) p. 42.
35. M. Green and J.W. Linnett, *J. Chem. Soc.* 1960, 4959.
36. M.E. Boyd, *J. Chem. Phys.* 37, 1317 (1962).
37. A.D. Walsh, *J. Chem. Soc.* 1953, 2288.
38. F.W. Dalby, *Can. J. Phys.* 36, 1336 (1958).
39. H. Margeneau and G.S. Murphy, The Mathematics of Physics and Chemistry, D. Van Nostrand Co., Inc., Princeton, N. J. (1956) p. 41.

40. A. Savitzky and M.J.E. Golay, Anal. Chem. 36, 1627 (1964); T.A. Brubaker and D.R. Stevens, J. Comput. Phys. 2, 465 (1968).
41. G.A. Cook, A.D. Kiffer, C.V. Klumpp, A.H. Malik, and L.A. Spence, "Separation of Ozone from Oxygen by a Sorption Press Process" in Ozone Chemistry and Technology Advances in Chemistry Advances in Chemistry Series No. 21 (1959) p. 44.
42. P.A. Giguere, J. Chem. Phys. 18, 88 (1950).
43. R.B. Holt, C.K. McLane, and O. Oldenberg, J. Chem. Phys. 16; 225, 638 (1948).
44. H.C. Urey, L.H. Dawsey, and F.O. Rice, J. Am. Chem. Soc. 51, 1371 (1929).
45. G. Gerzberg, Molecular Structure and Molecular Spectra I. Spectra of Diatomic Molecules, D. Van Nostrand Co., Princeton, N. J. (1950) p. 560.
46. E.D. Morris, Jr. (compare references 9 and 10) carried out the  $\text{Cl}_2 + \text{H}_2\text{O}_2$  study in this laboratory; present address: Ford Research Laboratory, Detroit, Michigan.
47. R.L. Redington, W.B. Olson, and P.C. Cross, J. Chem. Phys. 36, 1311 (1962).
48. G. Gerzberg, Molecular Structure and Molecular Spectra II. Infrared and Raman Spectra of Polyatomic Molecules, D. Van Nostrand Co., Princeton, N. J. (1945) p. 400.
49. G. Gerzberg, Molecular Structure and Molecular Spectra II. Infrared and Raman Spectra of Polyatomic Molecules, D. Van Nostrand Co., Princeton, N. J. (1945) p. 489.

50. S.L. Gerhard and D.M. Dennison, Phys. Rev. 43, 197 (1933).
51. M.K. Wilson and R.M. Badger, J. Chem. Phys. 16, 741 (1948).
52. N.S. Bayliss and E.G. McRae, J. Phys. Chem. 58, 1002 (1954); 61, 562 (1957).
53. I.A. Zhmyrev, V.V. Zelinski, V.P. Kolobkov, A.S. Kochemirovskii, and I.I. Reznikova, Opt. and Spect. 8, 214 (196 ).
54. I.A. Zhmyreva and I.I. Reznikova, Opt. and Spect. 10, 142 (1961).
55. N.G. Bakhshiev, Bull. Acad. Sci. USSR, Phys. 26, 1252 (1963).
56. E.M. Arnett and D. Hufford, J. Am. Chem. Soc. 88, 3140 (1966).
57. M.B. Ledger and P. Suppan, Spectrochimica Acta 23A, 641 (1967).
58. G.C. Pimentel and A.L. McClellan, The Hydrogen Bond, W.H. Freeman and Co., San Francisco (1960) p. 157.
59. N.G. Bakshiev, Optics and Spectroscopy 7, 29 (1959).
60. D.L. Baulch, D.D. Drysdale, and A.C. Lloyd, Critical Evaluation of Rate Data for Homogeneous Gas-Phase Reactions of Interest in High-Temperature Systems, School of Chemistry, The University, Leeds (1969) p. 39.

Table I. Quantities Used Evaluation of  $k_3$ , the  $\text{HO}_2 - \text{HO}_2$  Disproportionation Rate Constant

System	$(PQ)^{1/2}$ ( $\text{sec}^{-1}$ )	$\sigma_2 I$ ( $\text{sec}^{-1}$ )	$[\text{H}_2\text{O}_2]$ $\left(\frac{\text{molecules}}{\text{cm}^3}\right)$	P $\left(\frac{\text{molecules}}{\text{cm}^3 \text{ sec}}\right)$	PQ ( $\text{sec}^{-2}$ )	Q $\left(\frac{\text{cm}^3}{\text{molecule sec}}\right)$
Infrared System	5.55	$0.425 \times 10^{-3}$	$5.3 \times 10^{15}$	$0.45 \times 10^{13}$	30.8	$6.8 \times 10^{-12}$
Ultraviolet One Lamp	11.09	$0.8 \times 10^{-3}$	$1.13 \times 10^{16}$	$1.8 \times 10^{13}$	123.0	$6.8 \times 10^{-12}$
Ultraviolet Two Lamp	14.5	$1.6 \times 10^{-3}$	$8.5 \times 10^{15}$	$2.7 \times 10^{13}$	210.2	$7.8 \times 10^{-12}$

$$k_3 = Q/2 = 3.6 \pm 0.5 \times 10^{-12} \text{ cm}^3/\text{molecule}\cdot\text{sec}$$

Table II. Evaluation of the Absorption Cross-Section of HO<sub>2</sub> at its Absorption Maximum in the Ultraviolet

f (sec <sup>-1</sup> )	Frequency Normalized Amplitudes						$\Delta I/I$ f→0	P molecules cm <sup>3</sup> sec	Q cm <sup>3</sup> molecule·sec	$\Delta[H_2O_2]$ molecules cm <sup>3</sup>	$\sigma$ cm <sup>2</sup> /molecules Base e
	Observed		Limit as f→0								
	2000	2050	2100	2000	2050	2100					
Two Photolytic Lamps											
1/4	16519	17201	16391	17480	18202	17345					
1	14081	13550	14285	18725	18021	18996	$3.39 \times 10^{-3}$	$2.7 \times 10^{13}$	$7.1 \times 10^{-12}$	$1.95 \times 10^{12}$	$4.6 \times 10^{-18}$
2	9606	9798	9745	16010	16330	16242					
4	6373	7196	7146	14162	15991	15880					
One Photolytic Lamp											
1/4	11117	11653	12306	12491	13093	13827					
1	9392	9542	9625	13612	13892	13950	$2.65 \times 10^{-3}$	$1.8 \times 10^{13}$	$7.1 \times 10^{-12}$	$1.59 \times 10^{12}$	$4.4 \times 10^{-18}$

Table III. Modulation Spectrum in the Photolysis of Chlorine in the Presence of Hydrogen Peroxide

---

---

$\lambda\text{\AA}$	Amplitude	Phase Shift
2500	1593	-52.4°
2400	5494	-21.0°
2300	11629	-18.3°
2250	13947	-17.8°
2200	17258	-17.6°
2150	19279	-17.6°
2100	20496	-16.9°
2050	20650	-16.9°
2000	20205	-15.6°
1950	17644	-14.6°

---

---

Table IV. Moments of Inertia and Rotational Constants for Various Geometrical Configurations of HO<sub>2</sub>

H-O	Bond Lengths (Å)		Bond Angle (°)	Moments for Inertia ( $\times 10^{40}$ g-cm <sup>2</sup> )			Rotational Constants (cm <sup>-1</sup> )		
		O-O		I <sub>A</sub>	I <sub>B</sub>	I <sub>C</sub>	A	B	C
0.96		1.30	115	1.21	22.5	23.8	23.15	1.24	1.18
0.96		1.30	110	1.29	22.6	23.9	21.61	1.24	1.17
0.96		1.30	105	1.36	22.7	24.1	20.54	1.23	1.16
0.96		1.30	100	1.41	22.8	24.3	19.87	1.22	1.15
0.96		1.30	95	1.43	23.0	24.4	19.55	1.22	1.15
0.96		1.27	105	1.36	21.7	23.0	20.53	1.29	1.21
0.96		1.45	105	1.36	28.3	29.7	20.57	0.99	0.94

Table V. Infrared Absorption Frequencies of the Hydroperoxyl Radical

Workers	Phase	Absorption Frequencies $\text{cm}^{-1}$			Assignments
Milligan and Jacox	Argon Matrix at $4^\circ\text{K}$	3414	1389.5	1101	$\nu_1 \nu_2 \nu_3$
J.F. Ogilvie	Argon-Neon Matrix at $4^\circ\text{K}$	3412	1395	1104	$\nu_1 \nu_3 \nu_2$
Present Results	Gas Phase at $295^\circ\text{K}$	3410	1390	1095	see text

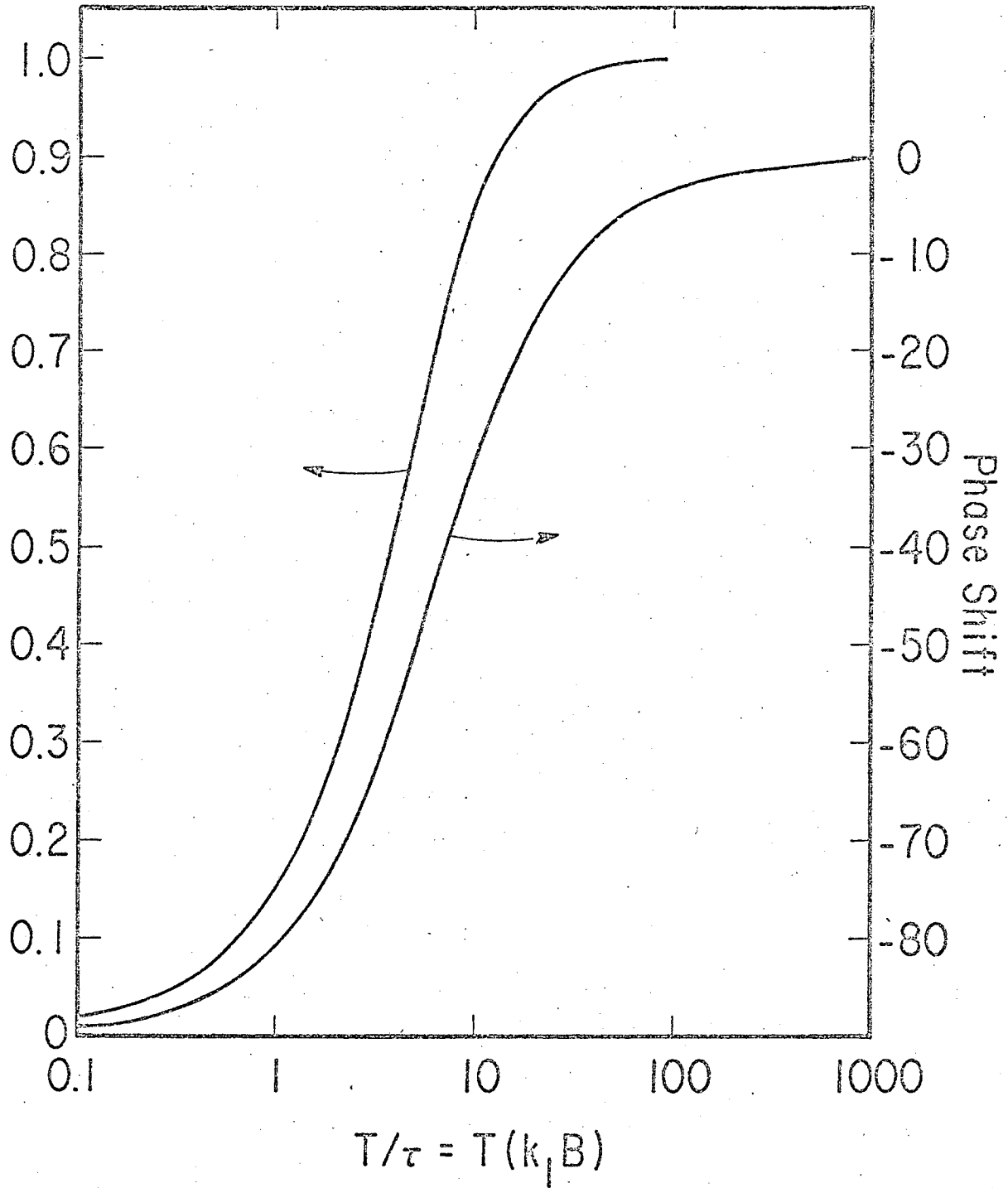
Titles to Figures

- Fig. 1. Dependence of the fundamental modulation frequency of a primary first-order radical on the ratio of flashing period to radical life-time. The amplitude is relative to the limiting amplitude as  $T/\tau$  approaches infinity.
- Fig. 2a. The dependence of the modulation of a secondary radical on the ratio of its life-time to the life-time of the preceding radical. a)  $\tau_2/\tau_1 = 0.01$ ; b)  $\tau_2/\tau_1 = 0.10$ ; c)  $\tau_2/\tau_1 = 1.00$ ; d)  $\tau_2/\tau_1 = 10$ ; e)  $\tau_2/\tau_1 = 100$ .
- Fig. 2b. Modulation amplitude relative to the limiting amplitude as  $T/\tau_1$  approaches infinity. a)  $\tau_2/\tau_1 = 0.01$ ; b)  $\tau_2/\tau_1 = 0.10$ ; c)  $\tau_2/\tau_1 = 1.00$ ; d)  $\tau_2/\tau_1 = 10$ ; e)  $\tau_2/\tau_1 = 100$ .
- Fig. 3. Concentration modulation of a second-order radical as a function of the ratio of flashing period to radical life-time. The amplitude is relative to the limiting amplitude as  $T/\tau$  approaches infinity.
- Fig. 4. Concentration modulation of the product of a second-order radical as a function of the ratio of the flashing period to life-time of the radical forming the product. Note the strong dependence of amplitude on  $T/\tau$ .
- Fig. 5. Absorption spectra of hydrogen peroxide and of water obtained in this laboratory by conventional spectroscopy.
- Fig. 6. The absorption spectrum of hydrogen peroxide.  $\odot$  = Literature (Refs. 43 and 44);  $\square$  = This laboratory by standard spectroscopic techniques.

- Fig. 7. The modulated absorption spectrum of the infrared region 1050 to 1150  $\text{cm}^{-1}$  obtained during the photolysis of ozone in the presence of hydrogen peroxide.
- Fig. 8a. The modulated absorption spectrum obtained during the photolysis of ozone in the presence of hydrogen peroxide at 1.4 Hz. Six repetitive scans at 12  $\text{cm}^{-1}$  resolution and a three-point curve smooth.
- Fig. 8b. The modulated absorption spectrum obtained during the photolysis of ozone in the presence of hydrogen peroxide at 1.4 Hz. Eleven repetitive scans at 8  $\text{cm}^{-1}$  resolution and a three-point curve smooth.
- Fig. 9. The modulated absorption spectrum obtained during the photolysis of ozone in the presence of hydrogen peroxide at 1.4 Hz. The spectrum is the average of sixteen sweeps and a three-point curve smooth.
- Fig. 10. Infrared spectra from 1000 to 1150  $\text{cm}^{-1}$  obtained during the photolysis of hydrogen peroxide at 1 Hz.
- Fig. 11. The modulated infrared absorption between 1350 and 1520  $\text{cm}^{-1}$  obtained during the photolysis of hydrogen peroxide at 1 Hz. The spectrum is the average of 12 scans and a five-point curve smooth.
- Fig. 12 a-d. The progressive enhancement of the spectrum in Fig. 13 resulting from repetitive sweeps and curve smoothing.
- 12a. One scan; no curve smooth.
  - 12b. Seven scans; no curve smooth.
  - 12c. Twelve scans; no curve smooth.
  - 12d. Twelve scans; five-point curve smooth.

- Fig. 13. Phase shift of the infrared absorption peaks as a function of flashing period.  $\times = 1075 \text{ cm}^{-1}$ ;  $\circ = 1120 \text{ cm}^{-1}$ ;  $\square = 1373 \text{ cm}^{-1}$ ;  $\Delta = 1420 \text{ cm}^{-1}$ ;  $\odot =$  Average of all points.
- Fig. 14. The modulated ultraviolet absorption spectrum obtained during the photolysis of hydrogen peroxide by one lamp at 1/4 Hz.
- Fig. 15. The dependence of the phase shift of the modulation at 2200 Å on flashing period. The curve is the calculated curve for a primary second-order radical. Only one photolysis lamp was used.
- Fig. 16. Comparison of radical and reactant amplitudes extracted from the data with the amplitudes predicted by the mechanism.  $\circ =$  Radical amplitude;  $\square =$  Reactant amplitude. Solid curves are the amplitudes predicted by the mechanism.
- Fig. 17. The modulated absorption phase shifts from 2450 to 2000 Å obtained during the photolysis of hydrogen peroxide by two lamps.  $\circ = 1/4 \text{ Hz}$ ;  $\Delta = 1/2 \text{ Hz}$ ;  $\blacksquare = 1 \text{ Hz}$ ;  $\blacktriangle = 2 \text{ Hz}$ ;  $\odot = 4 \text{ Hz}$ ;  $\blacklozenge = 8 \text{ Hz}$ ;  $\square = 16 \text{ Hz}$ .
- Fig. 18. The modulated absorption amplitudes from 2450 to 2000 Å obtained during the photolysis of hydrogen peroxide by two lamps.  $\circ = 1/4 \text{ Hz}$ ;  $\Delta = 1/2 \text{ Hz}$ ;  $\blacksquare = 1 \text{ Hz}$ ;  $\blacktriangle = 2 \text{ Hz}$ ;  $\odot = 4 \text{ Hz}$ ;  $\blacklozenge = 8 \text{ Hz}$ ;  $\square = 16 \text{ Hz}$ .
- Fig. 19. The phase shift of the radical vs the flashing period. The curve is the calculated curve for a primary second-order radical.

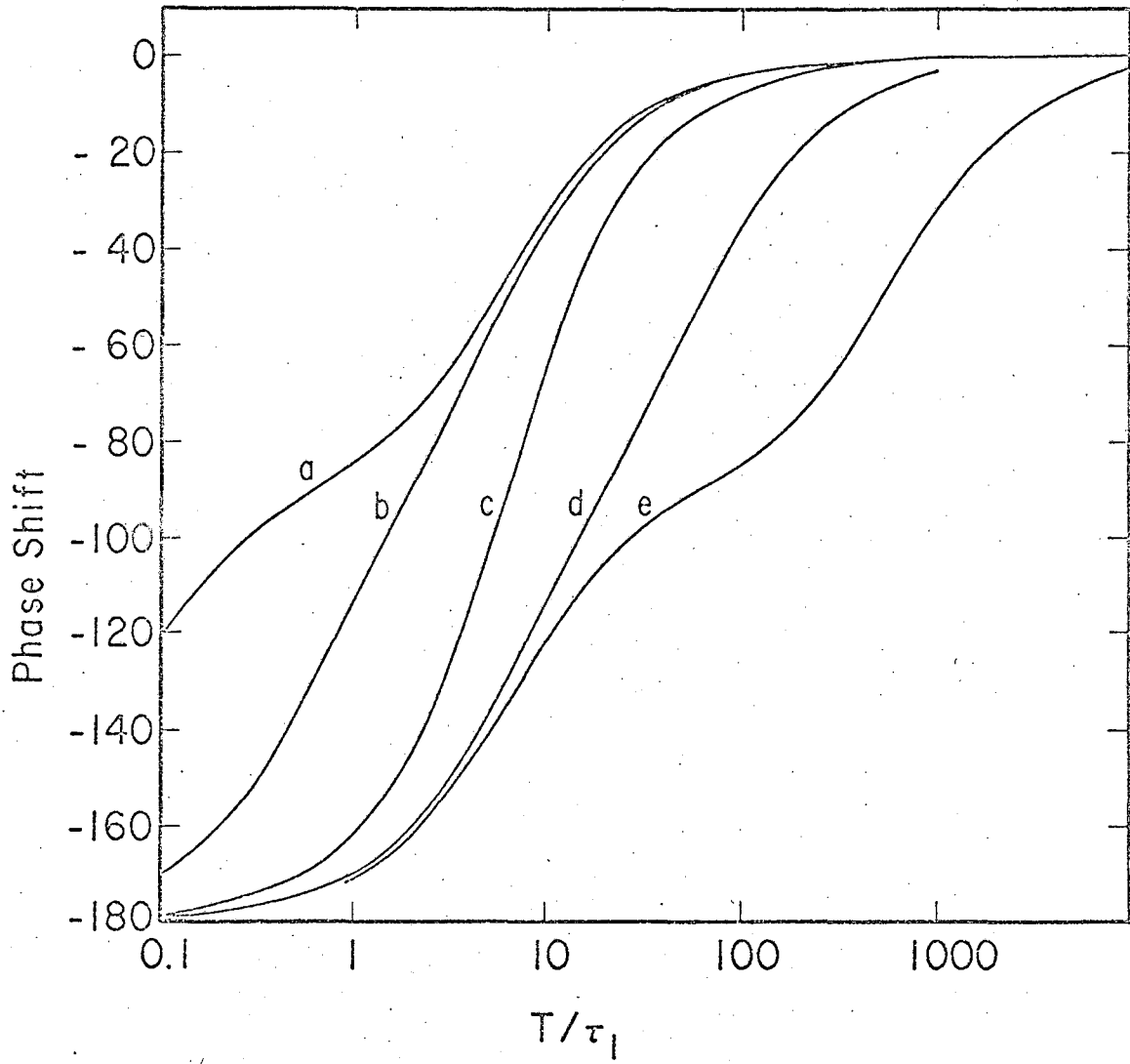
Fig. 20. The ultraviolet spectrum of the hydroperoxyl radical,  
 $-dI = \sigma I L dN$ .  $\odot$  = Average of all the ultraviolet spectra  
obtained from the photolysis of hydrogen peroxide  
at 2537 Å;  $\Delta$  = The spectrum from the photolysis of  
chlorine in the presence of hydrogen peroxide at  
3600 Å.



XBL 6910 -5903

Fig. 1

FIG. 1



XBL 6910-5905

Fig. 2a

FIG. 2

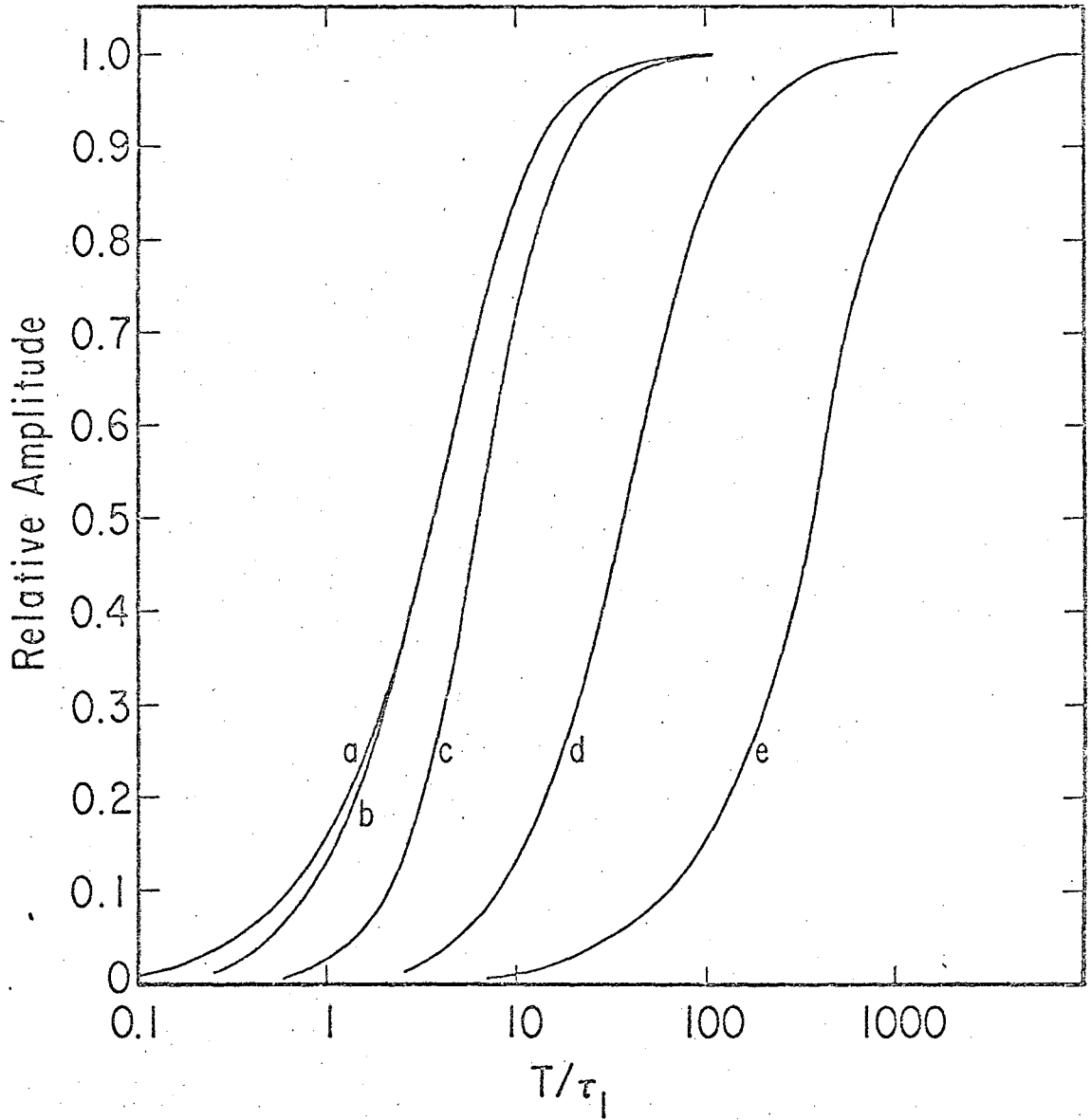
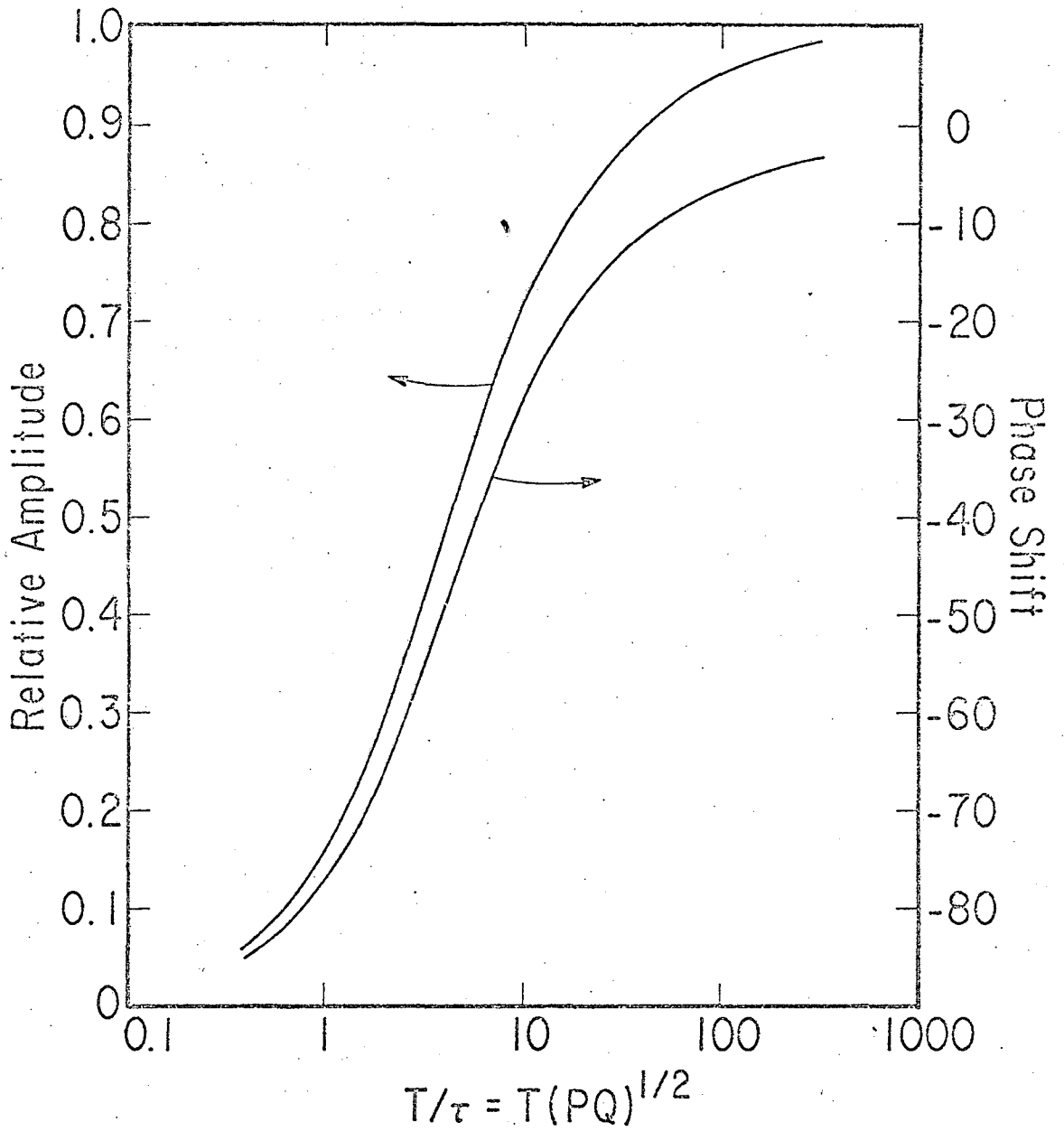


Fig. 2b

XBL 6910-5907

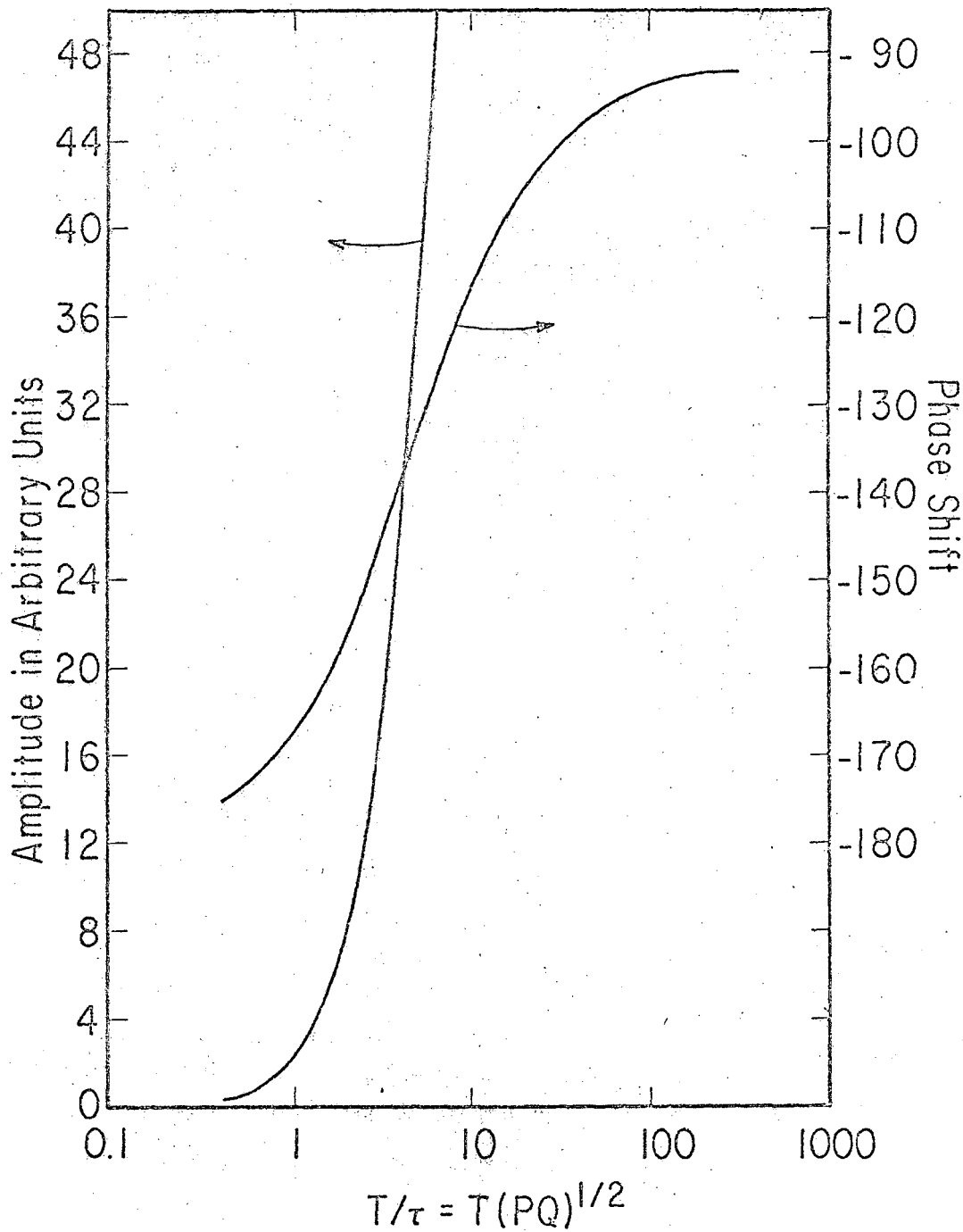
FIG. 2



XBL 6910-5909

Fig. 3

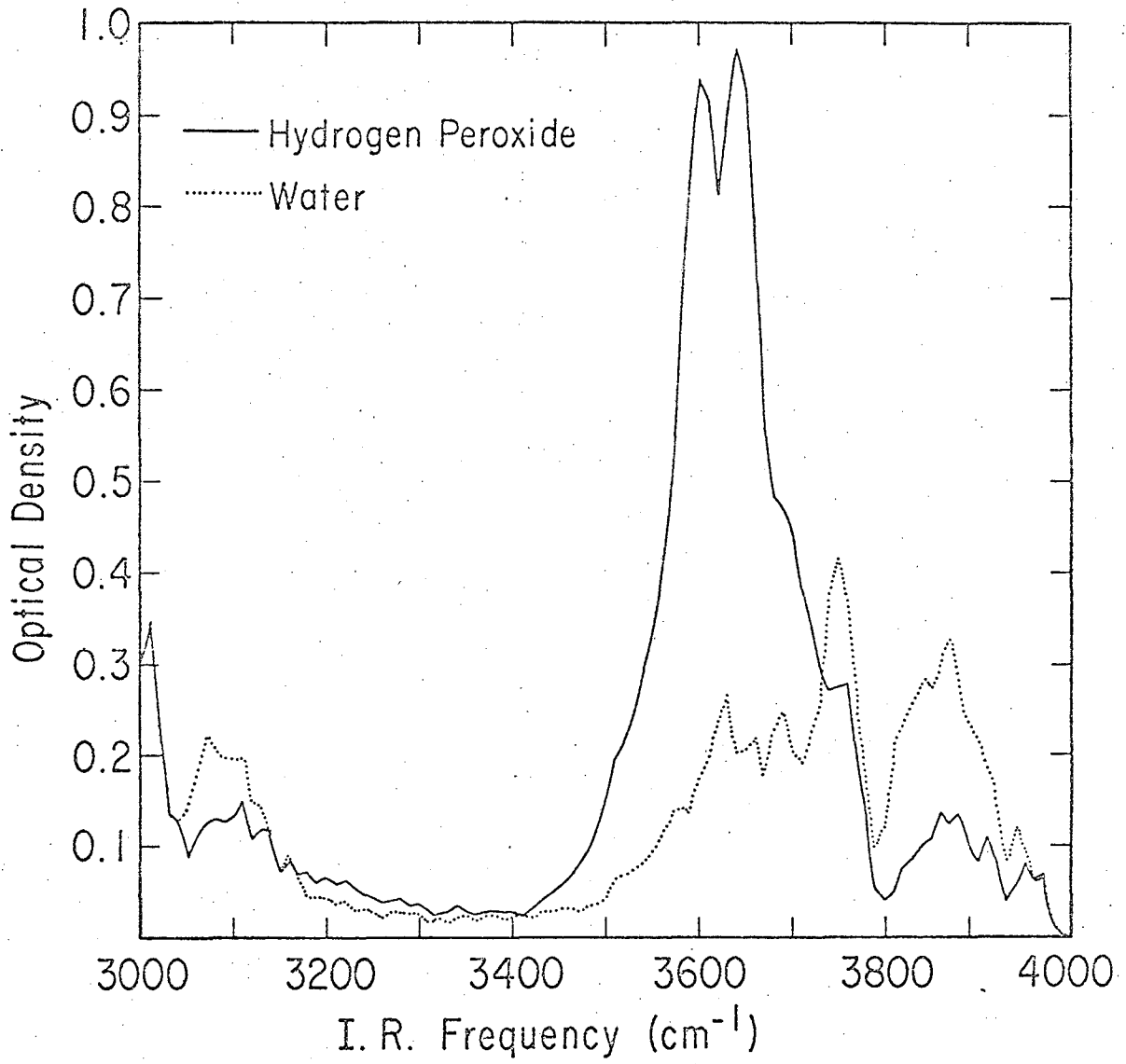
FIG. 3



XBL 6910-5906

Fig. 4

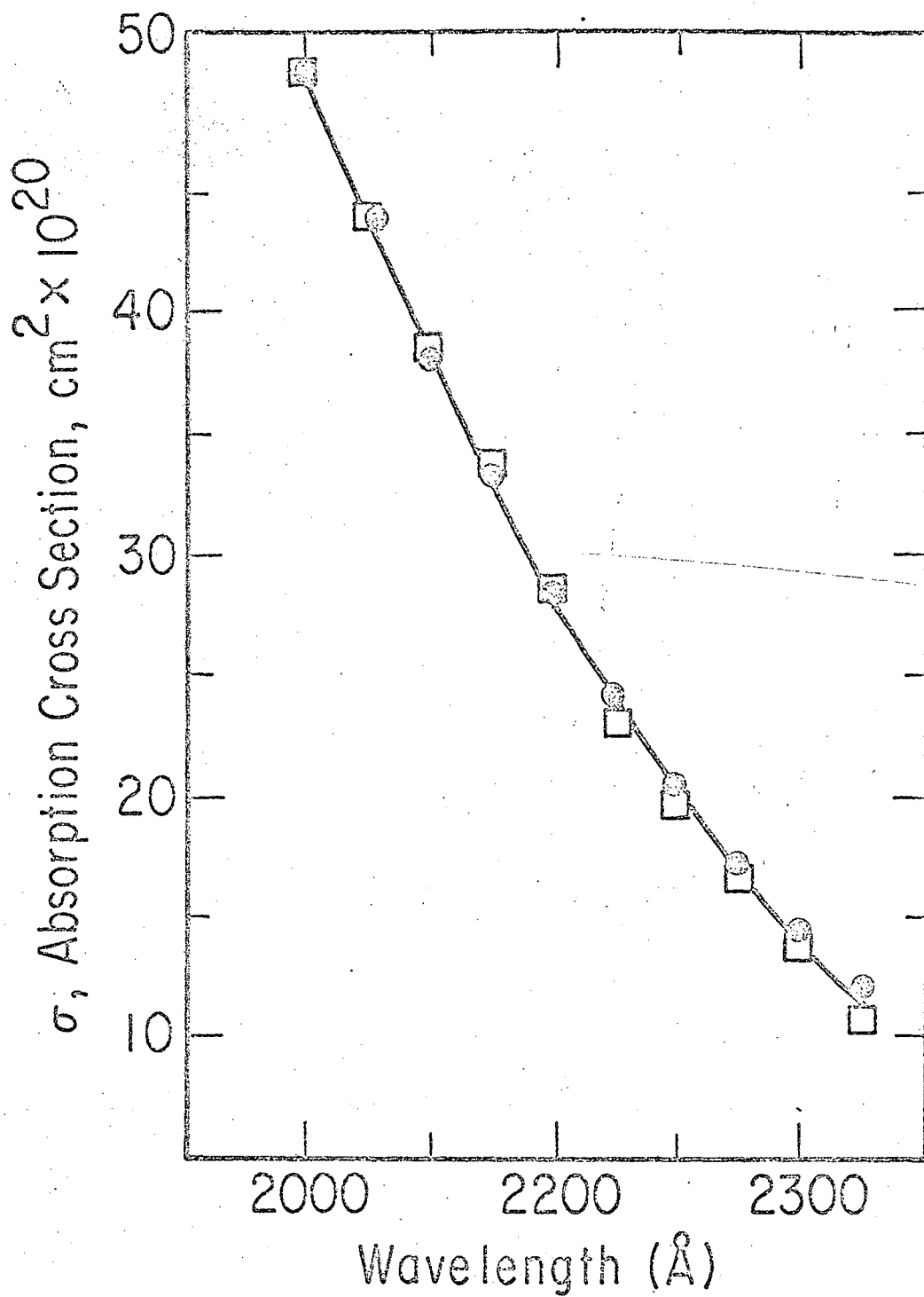
FIG. 4



XBL 6910 - 5908

Fig. 5

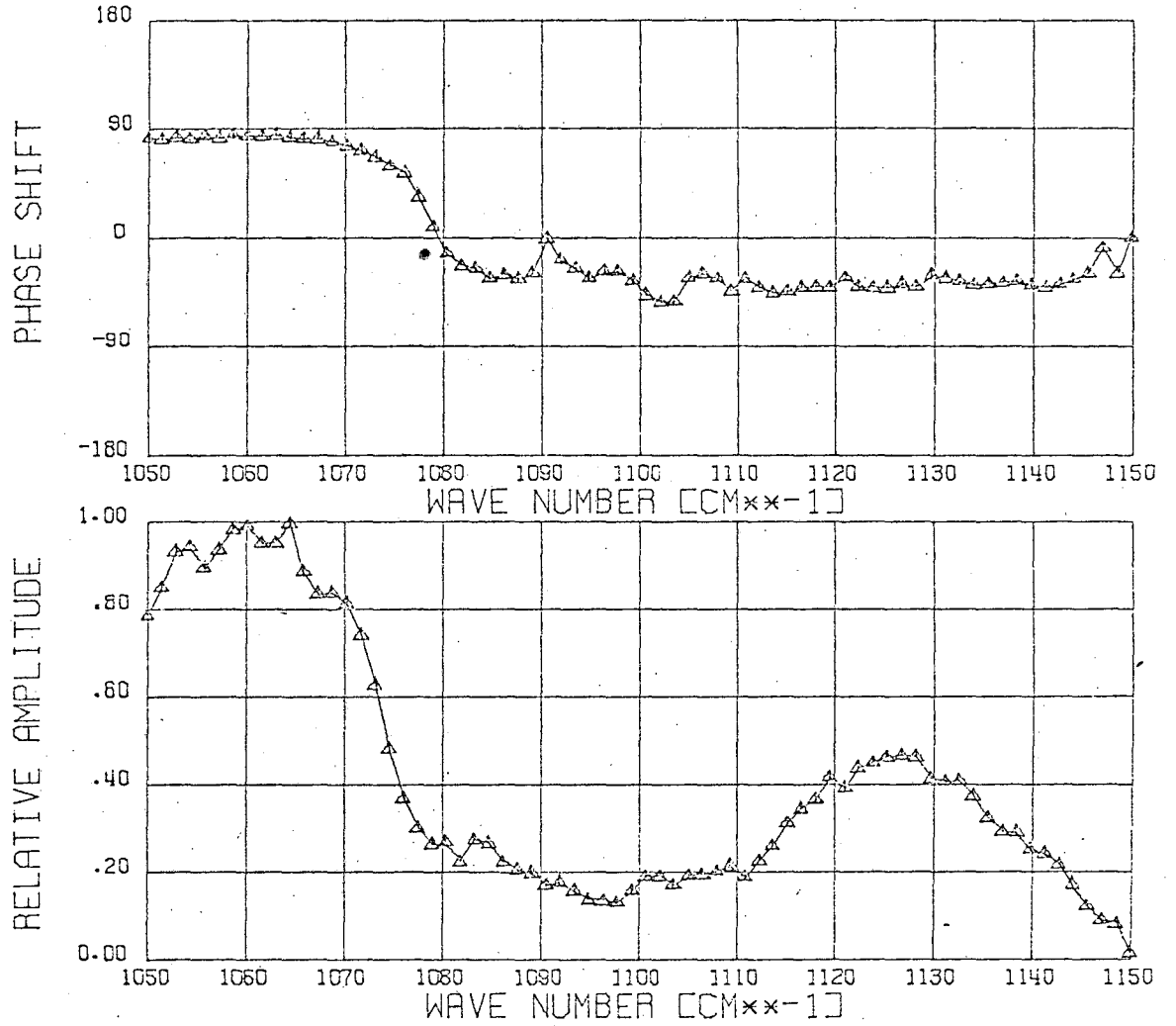
FIG. 5



XBL6910-5895

Fig. 6

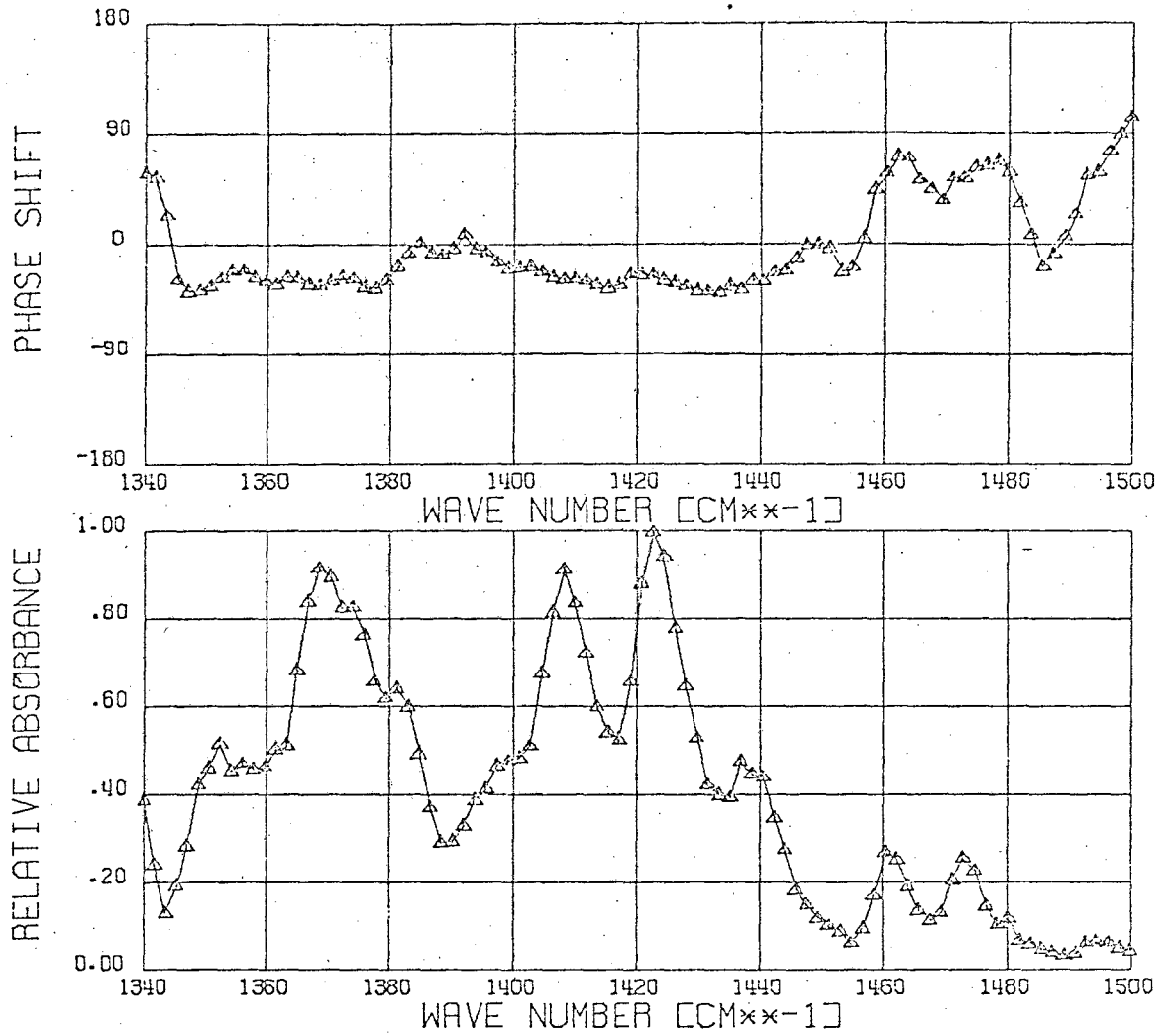
FIG. 6



XBL 6910-5503

Fig. 7

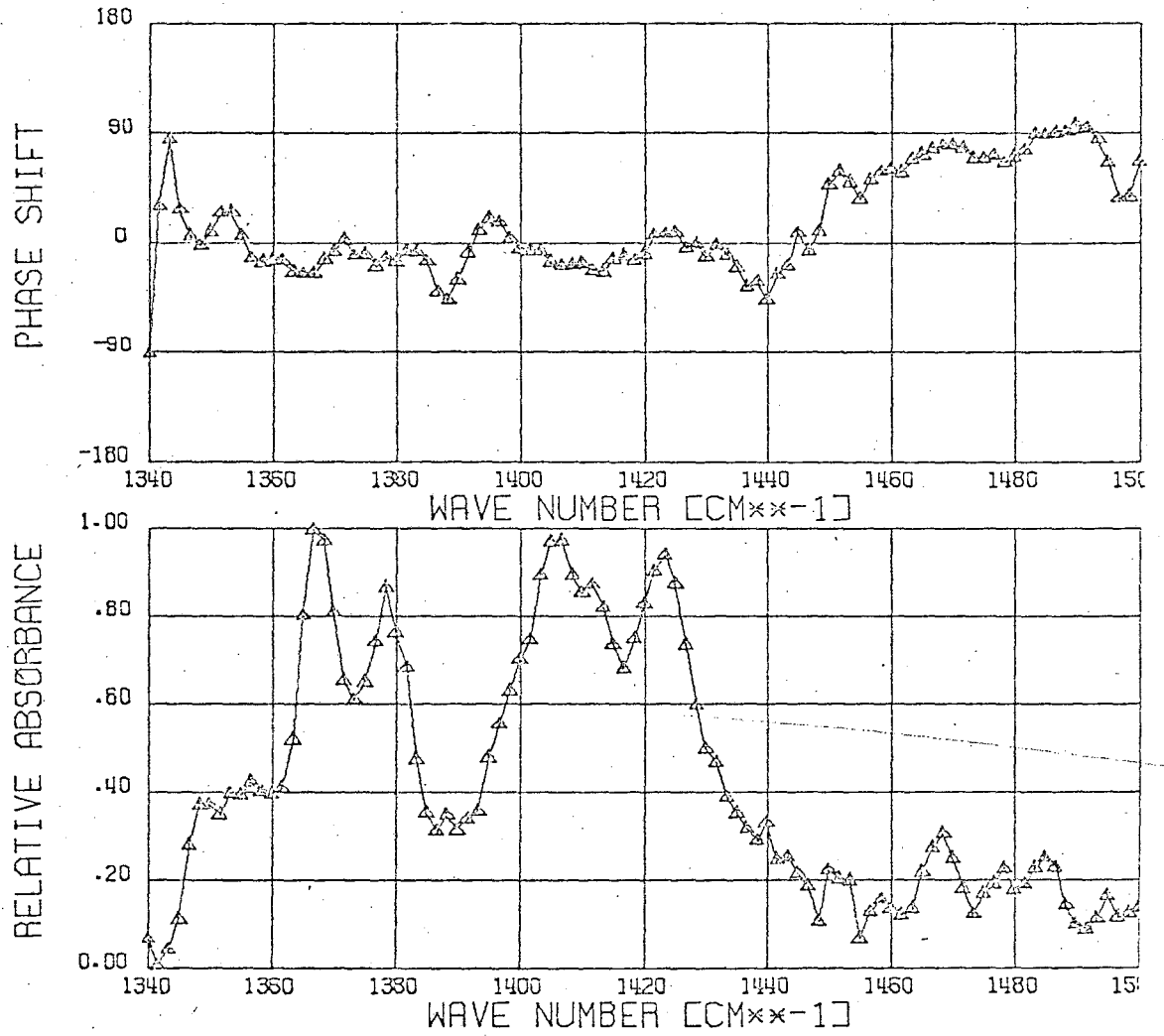
FIG. 7



XBL 6910-5762

Fig. 8a

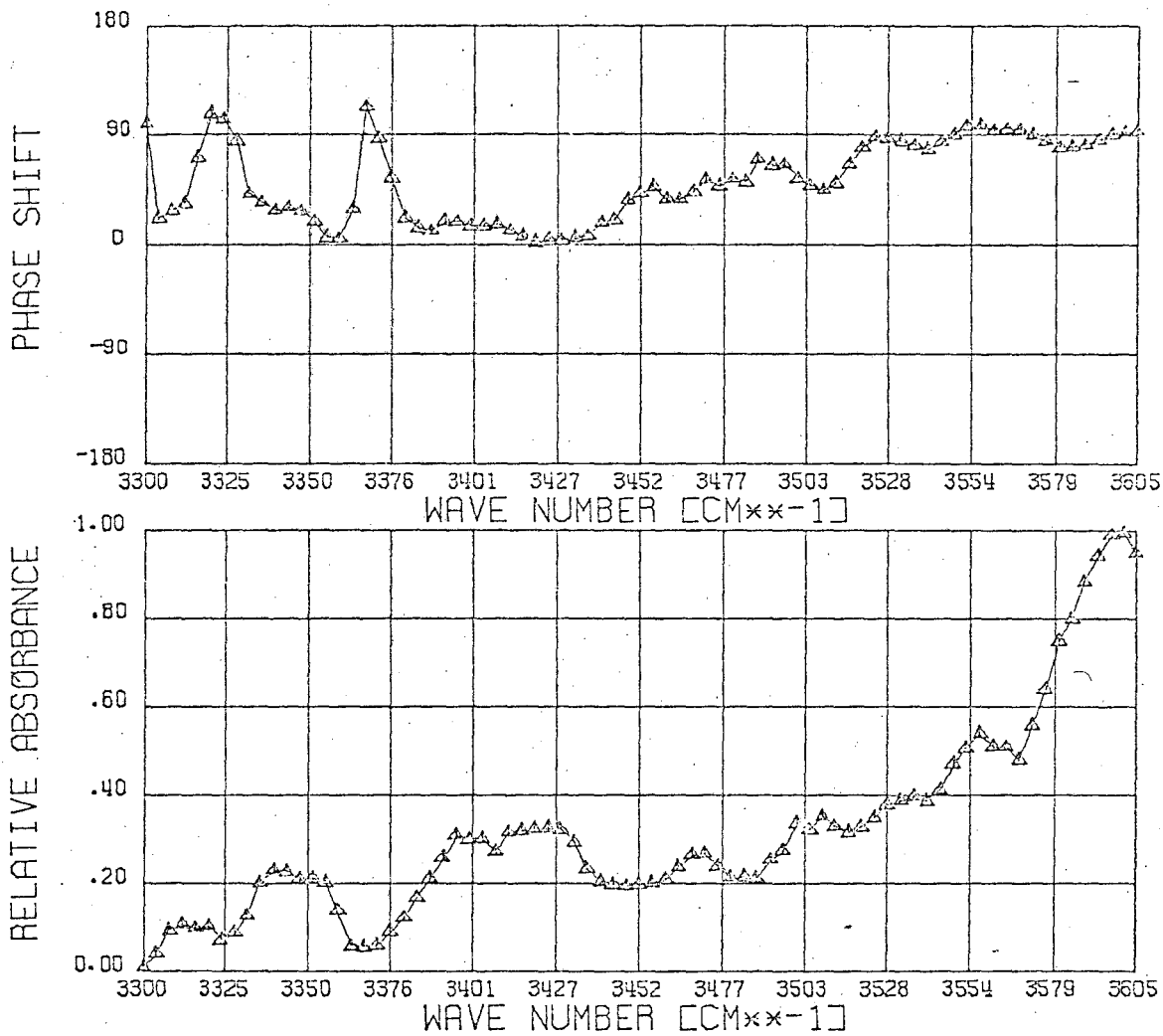
FIG. 8A



XSL 6910-5

Fig. 8b

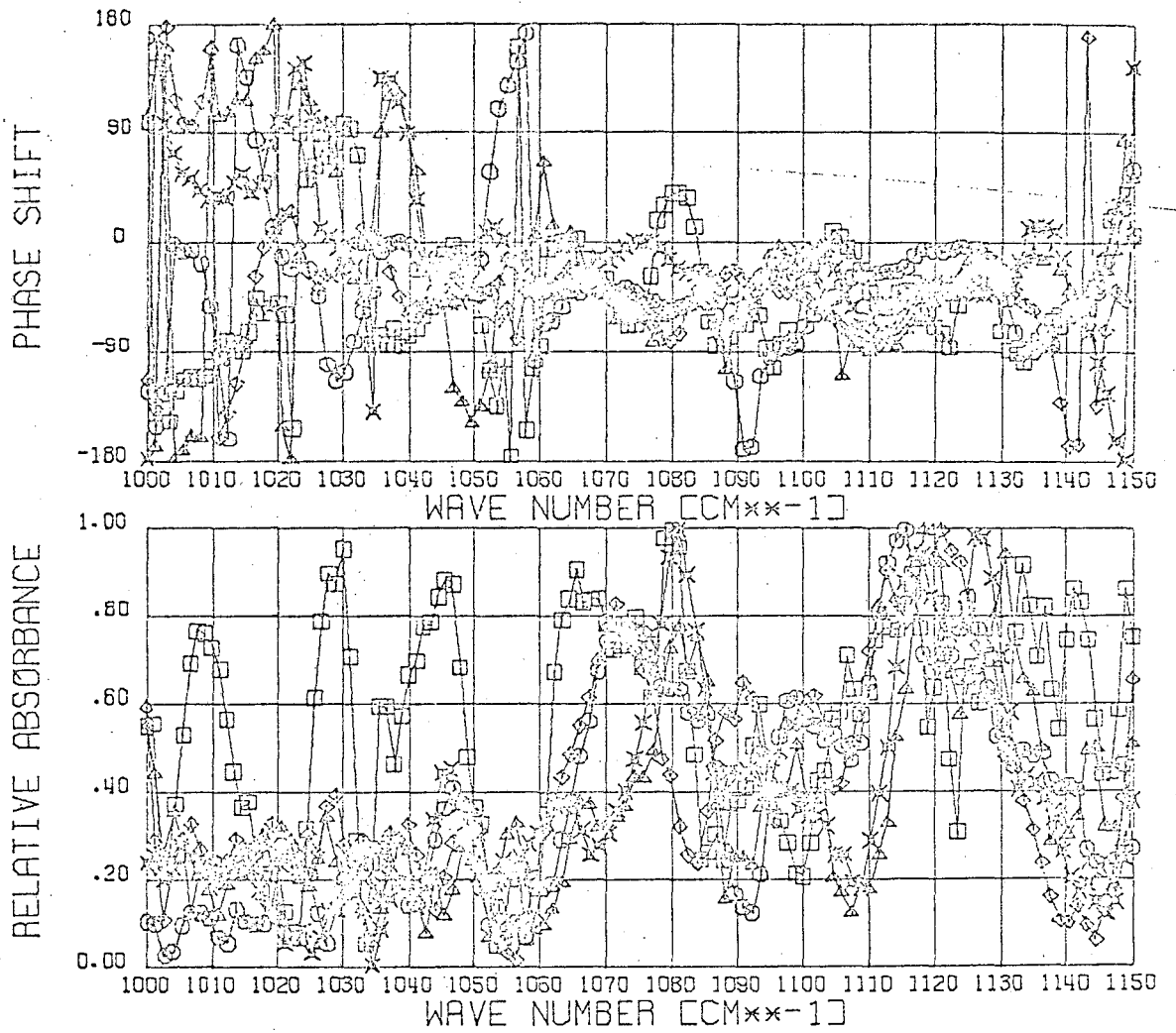
FIG. 8B



XBL 6910-5761

Fig. 9

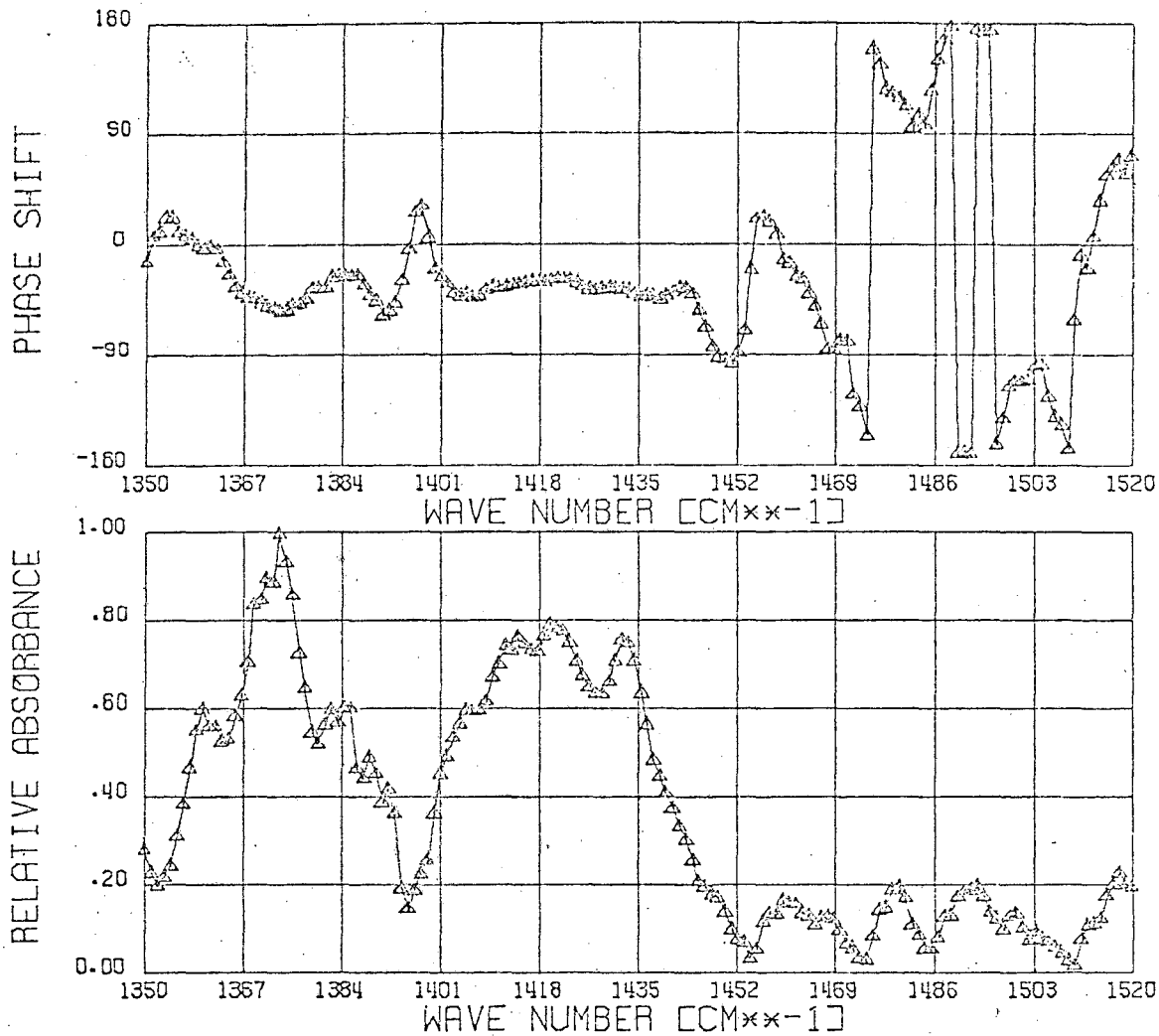
FIG. 9



XBL 6910-5802

Fig. 10

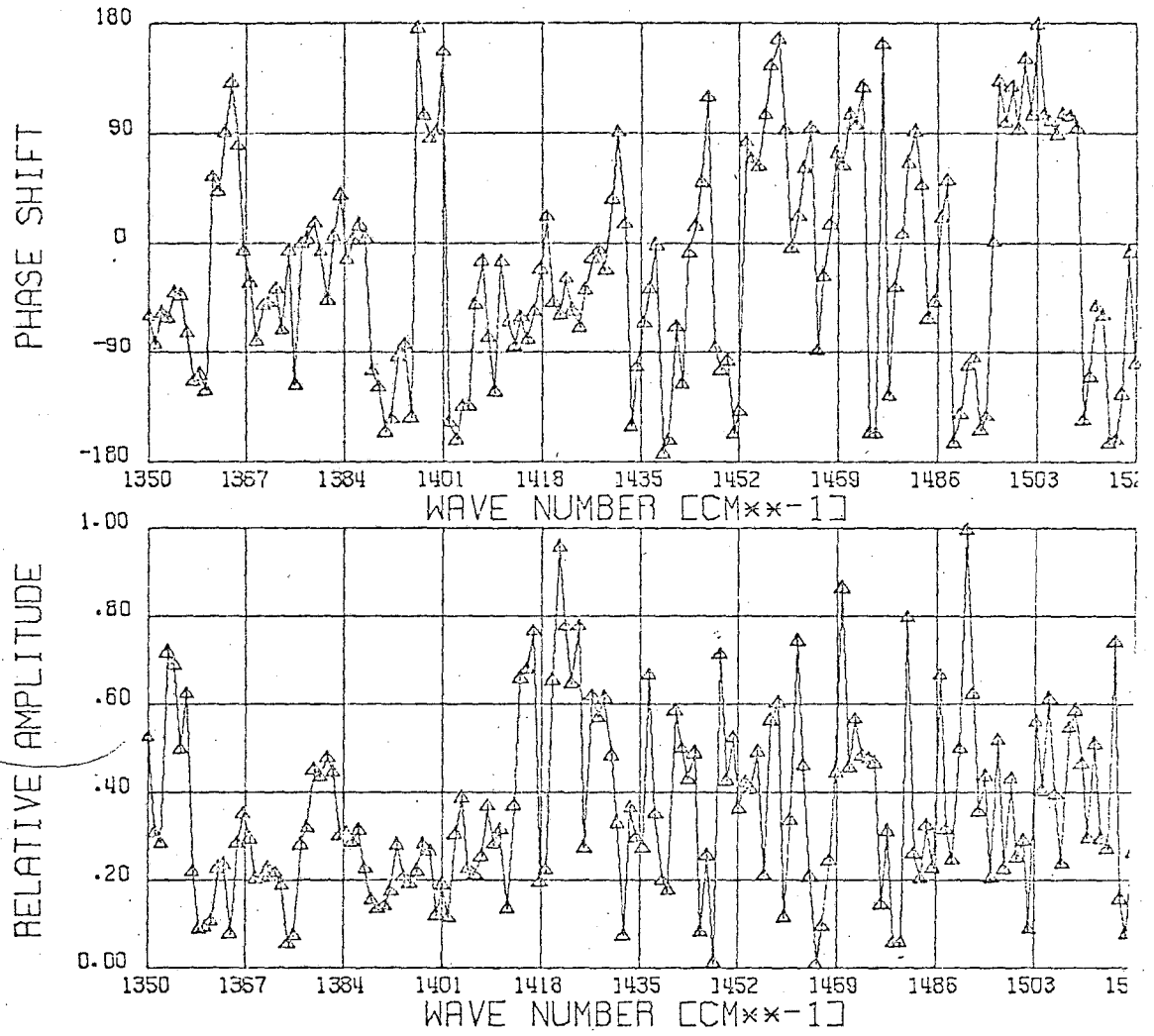
FIG. 10



XBL 6910-5765

Fig. 11

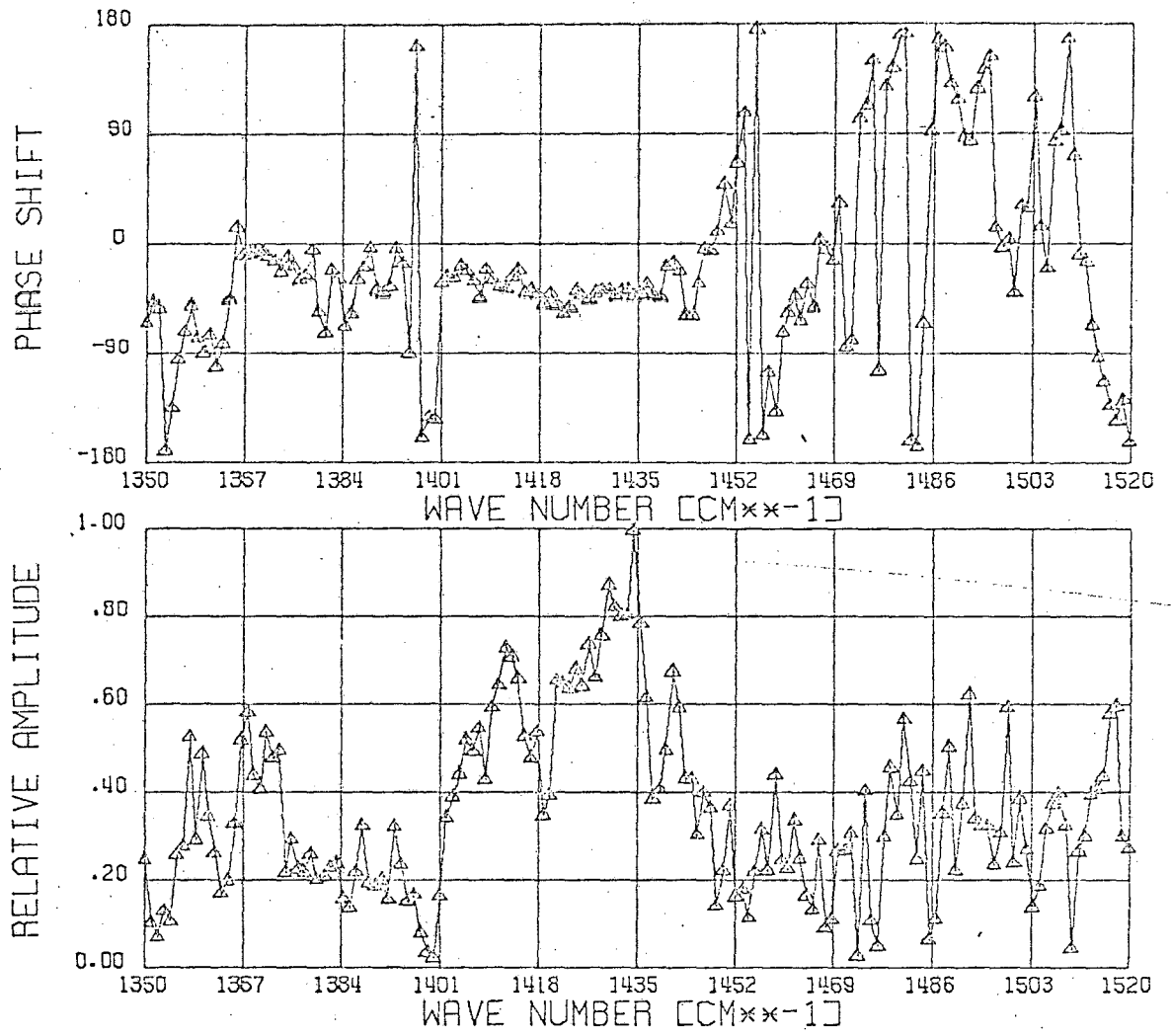
FIG. 11



XBL 6910-5

Fig. 12a

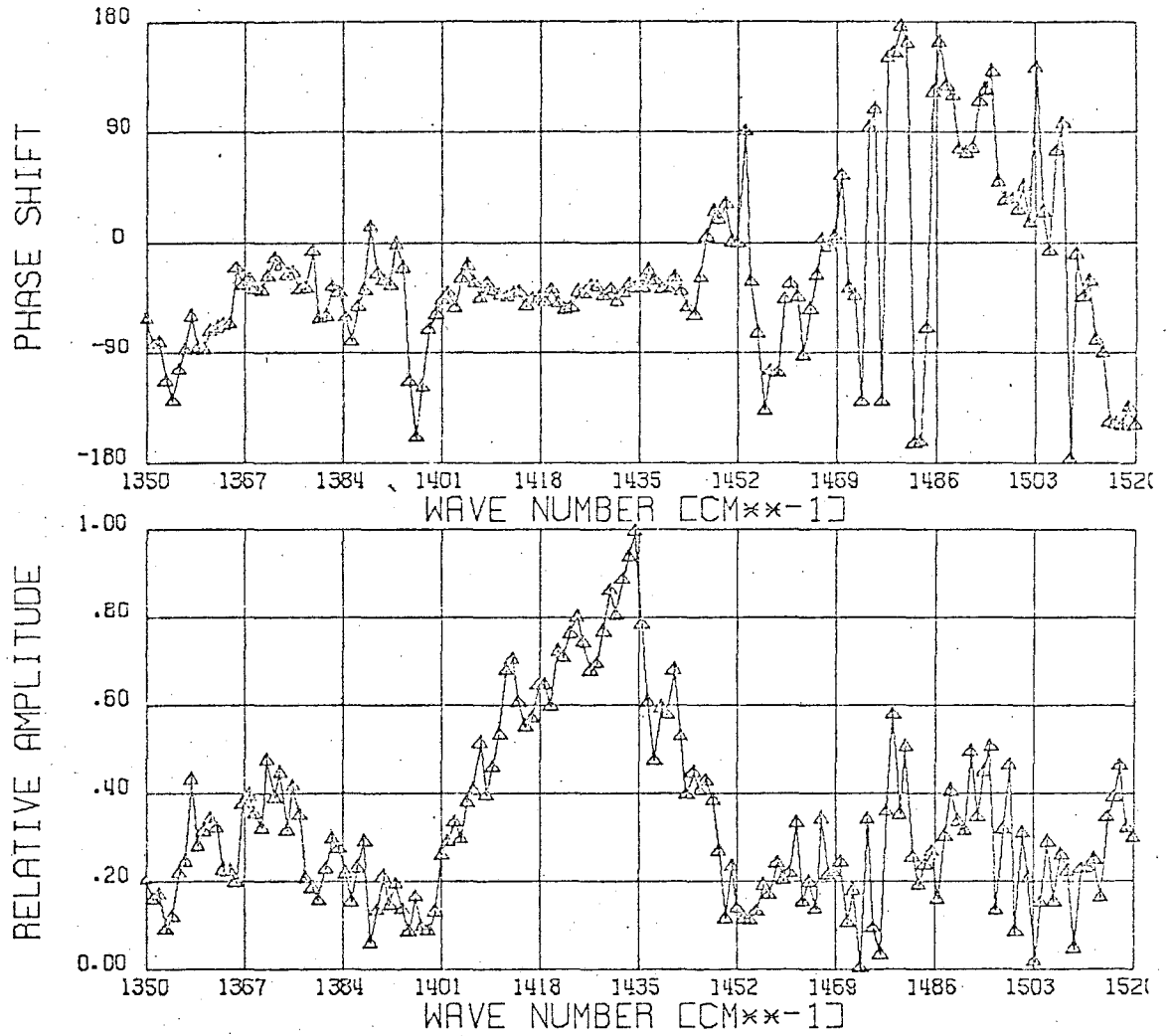
FIG. 12A



XBL 6910-5763

Fig. 12b

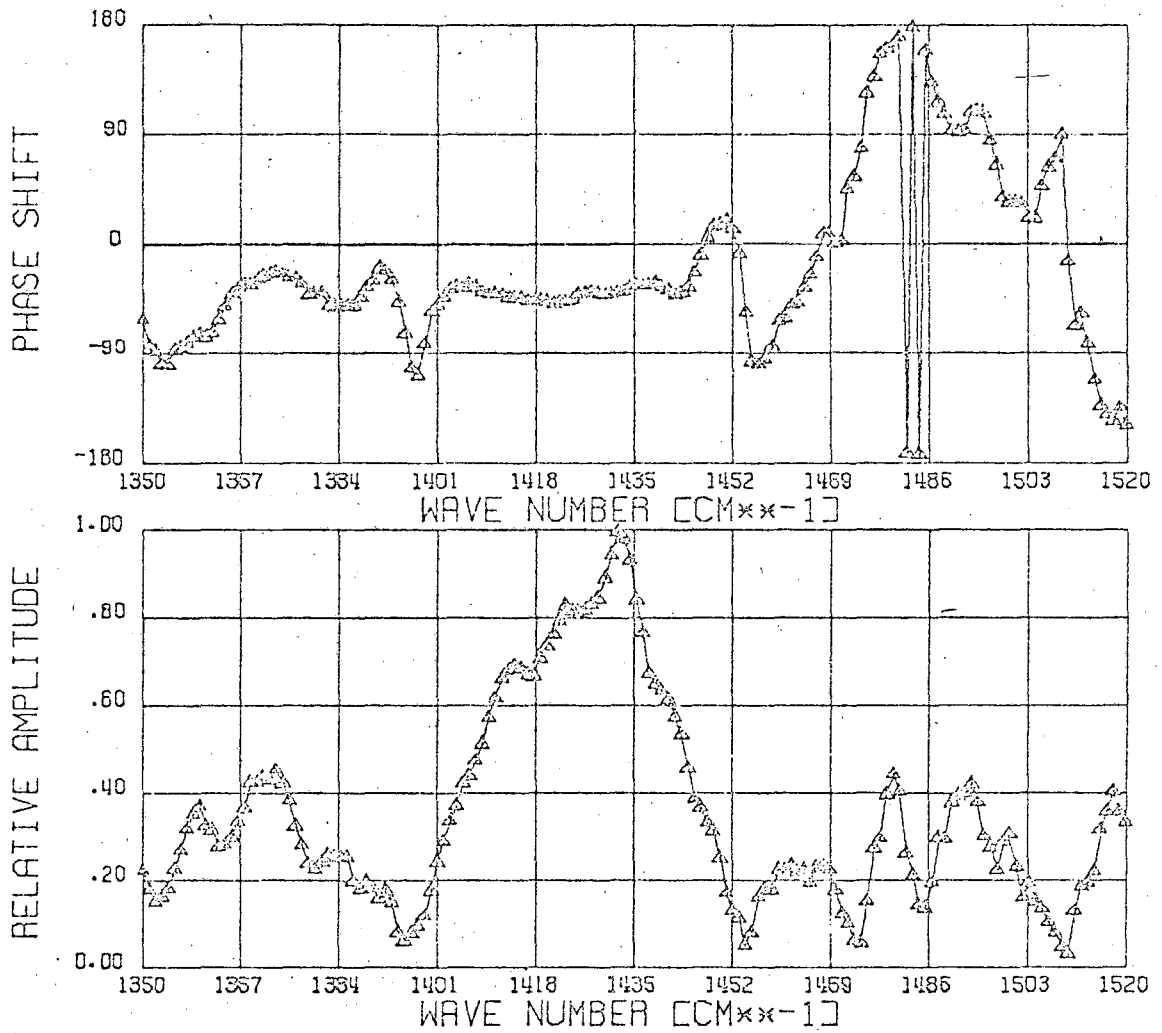
FIG. 12 B



XPL 6910-576

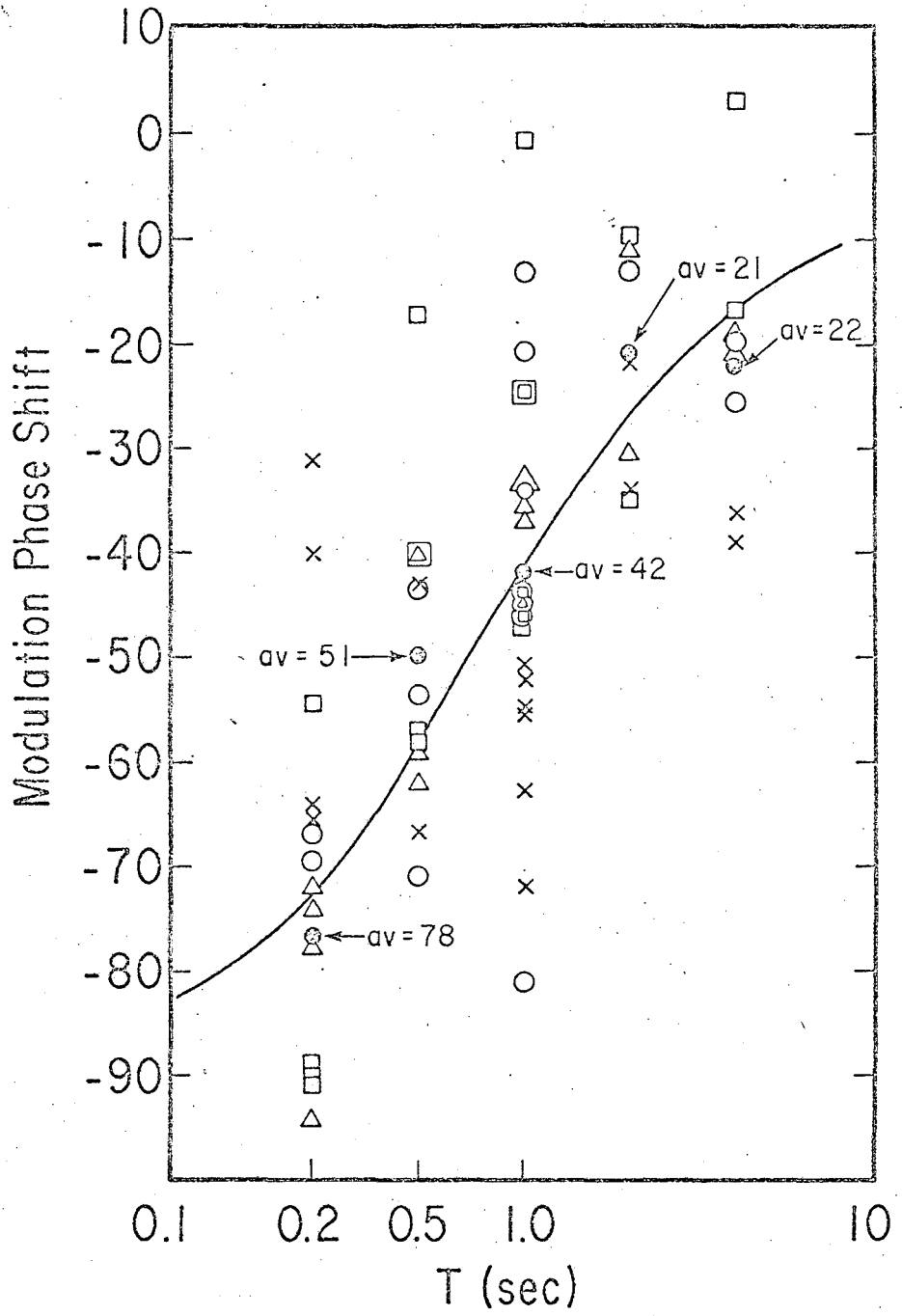
Fig. 12c

FIG. 12 C



XBL 6910-5766

Figure 12d.

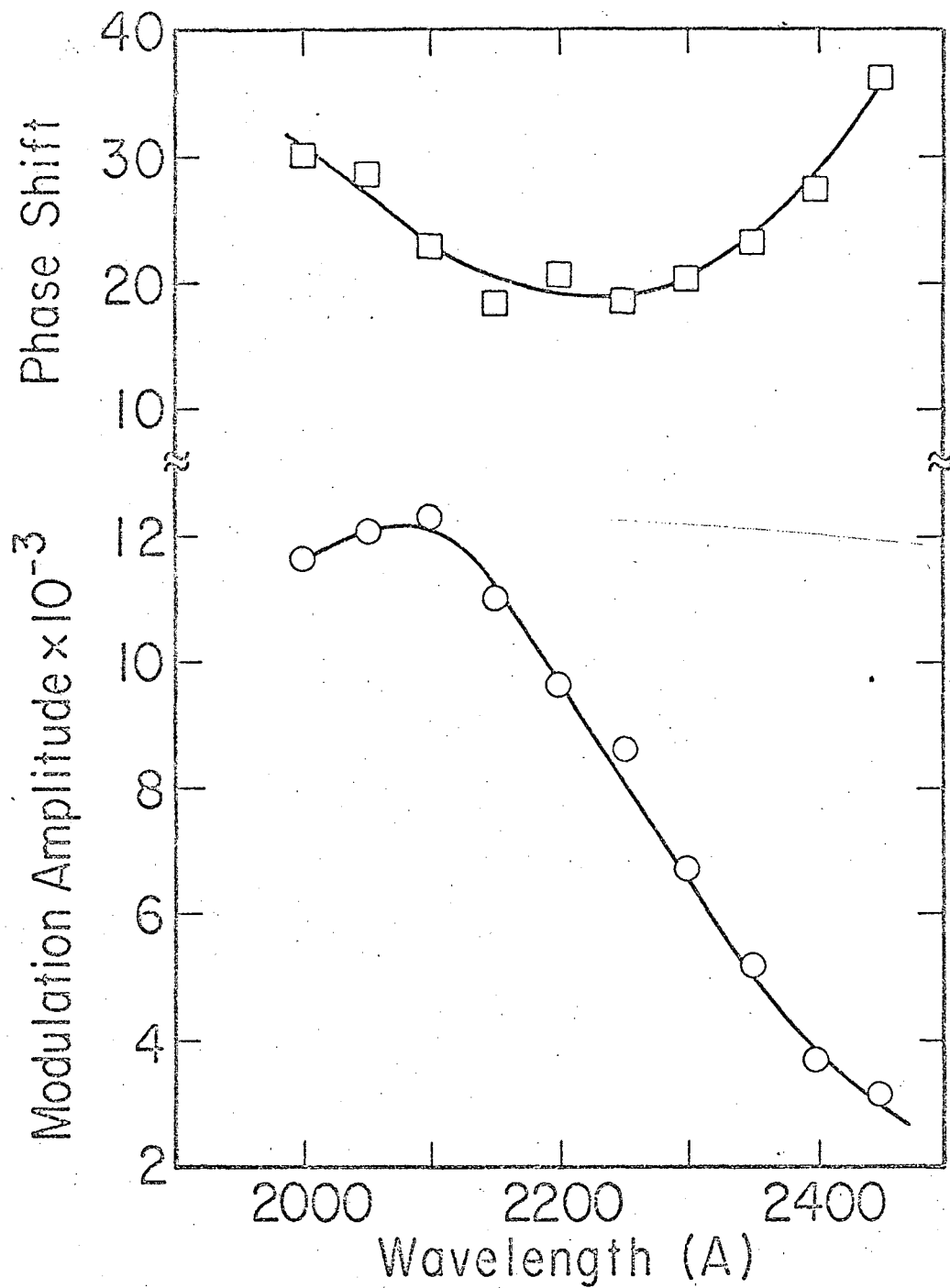


XBL 6910-5899

Fig. 13

FIG

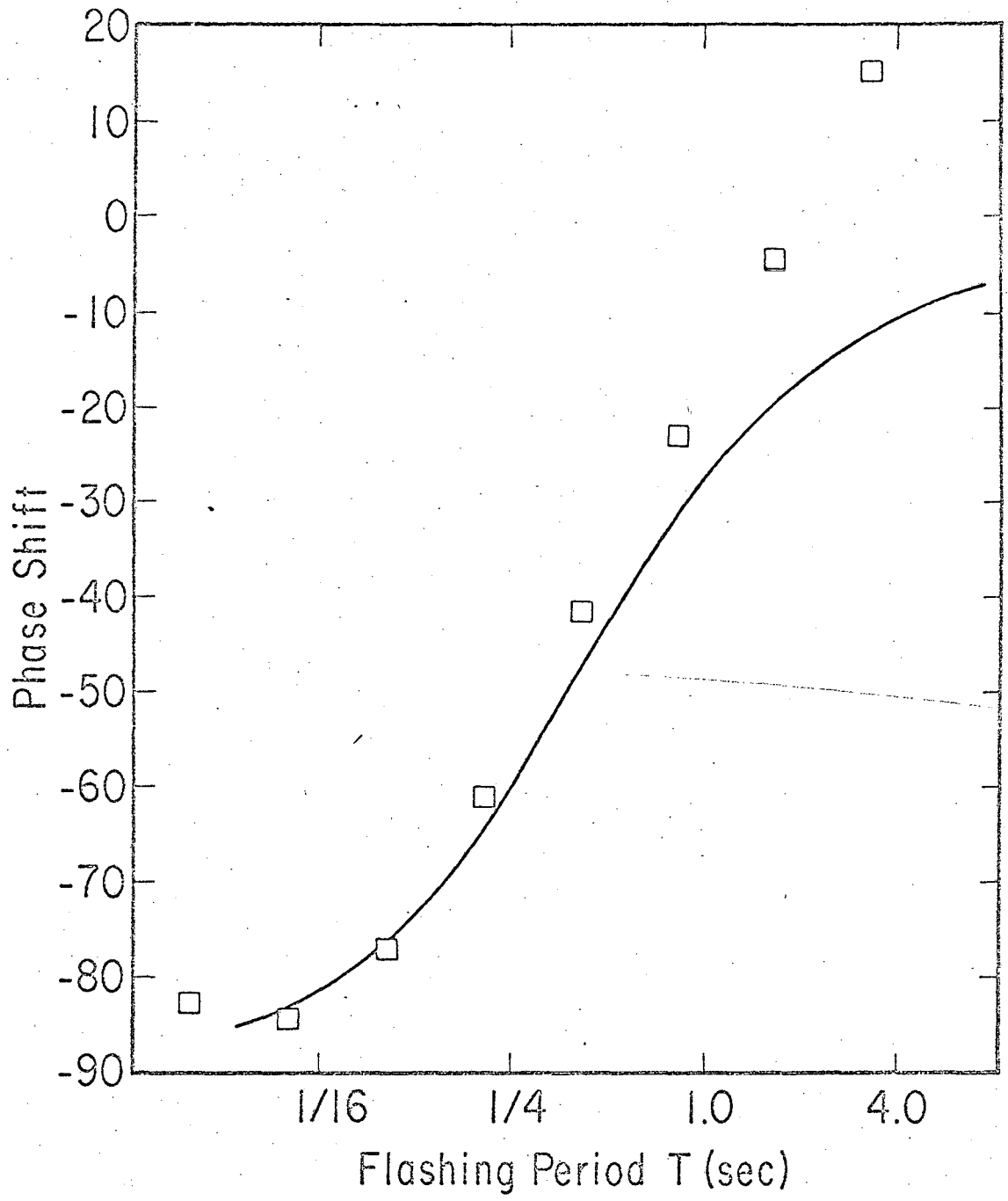
13



XBL 6910-5897

Fig. 14

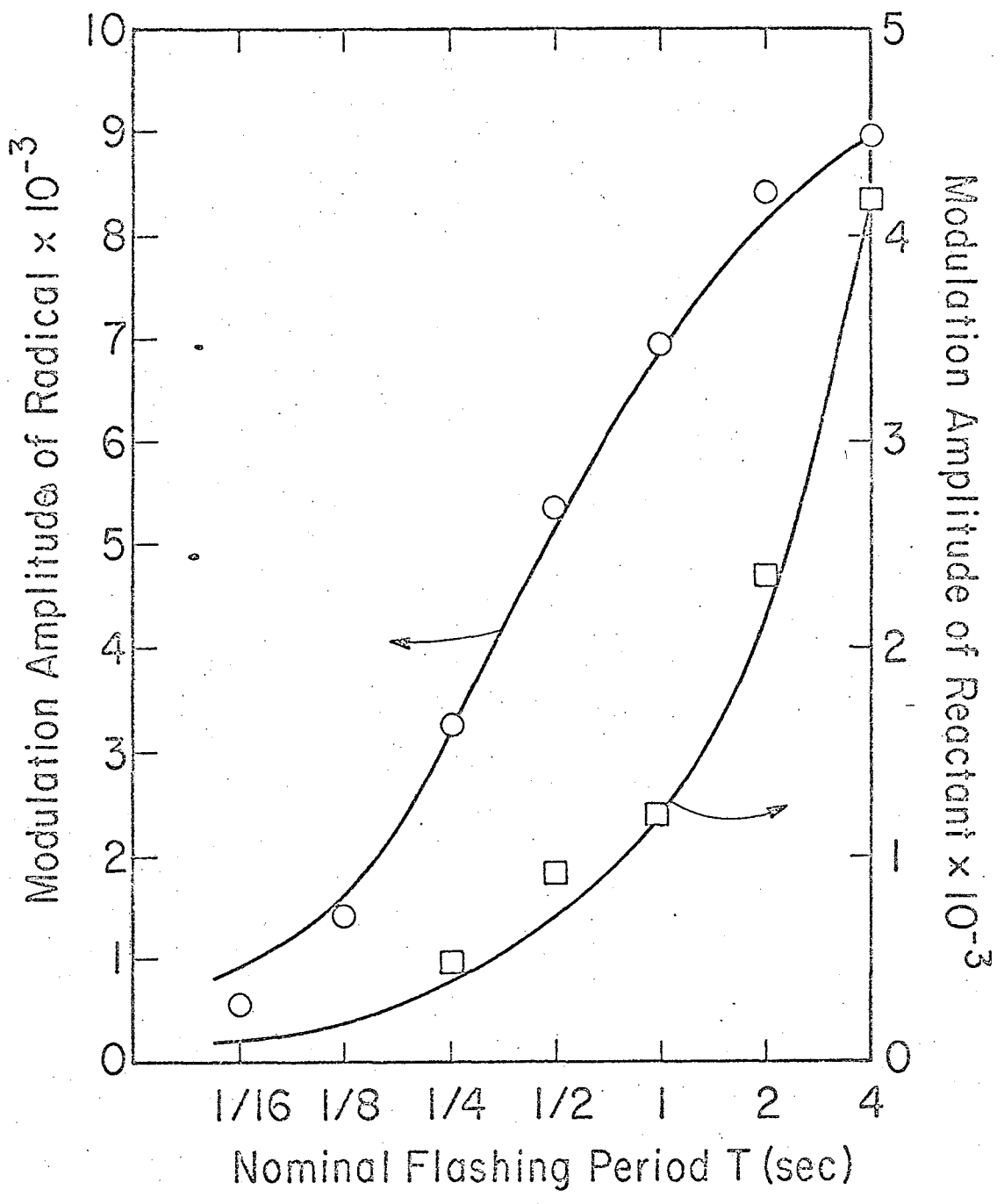
FIG 14



XBL 6910-5900

Fig. 15

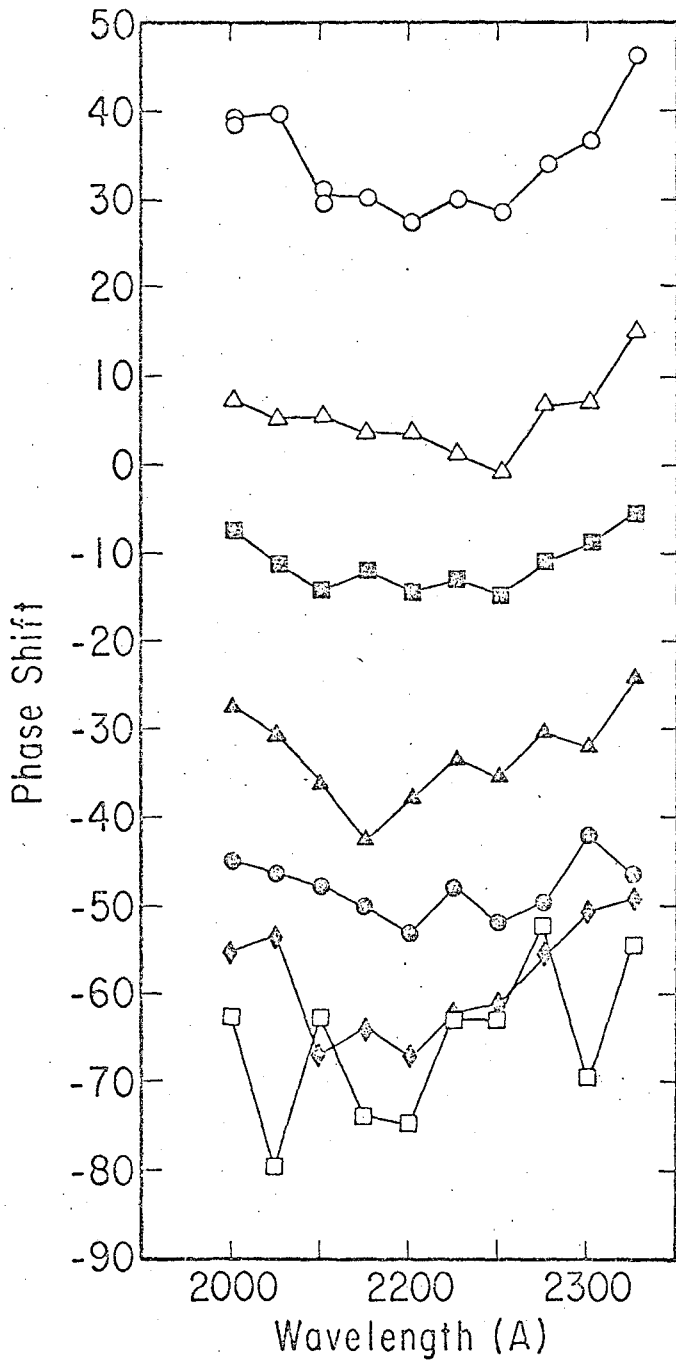
FIG 15



XBL 6910 - 5904

Fig. 16

FIG 16

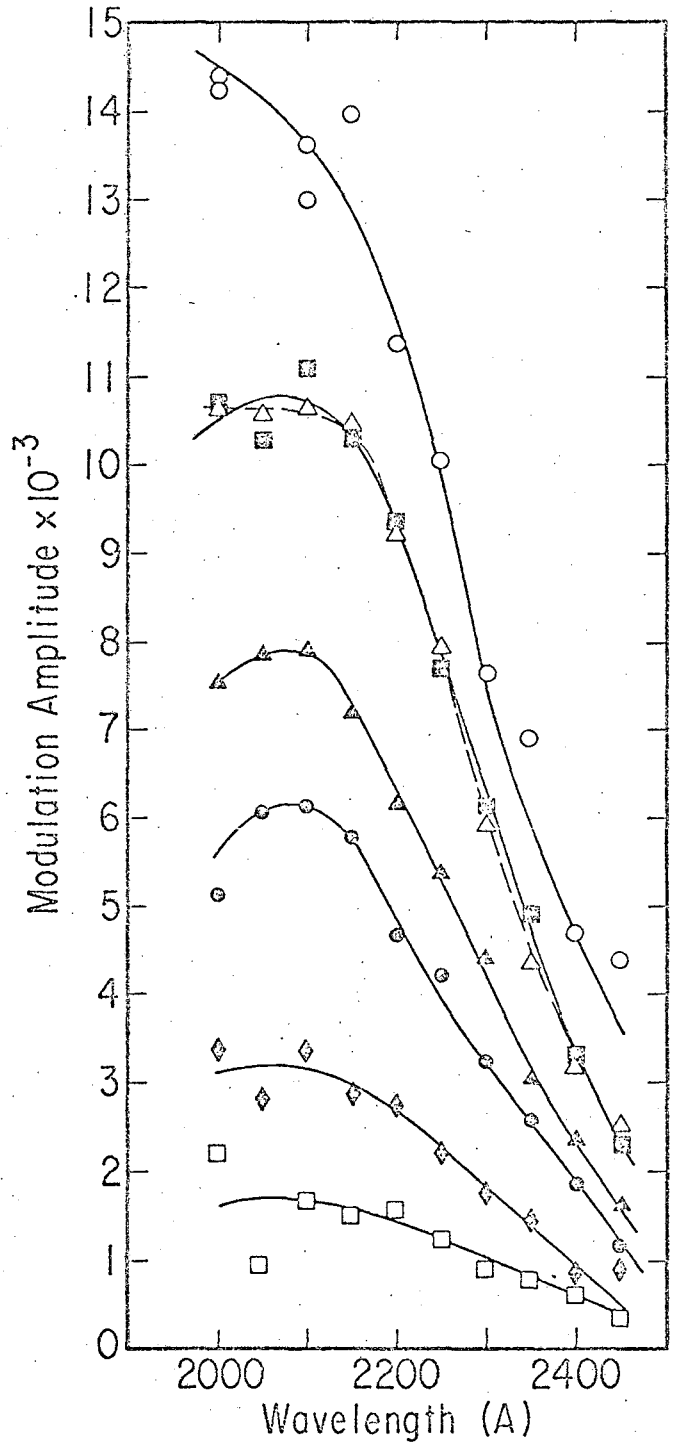


XBL 6910-5910

Fig. 17

FIG

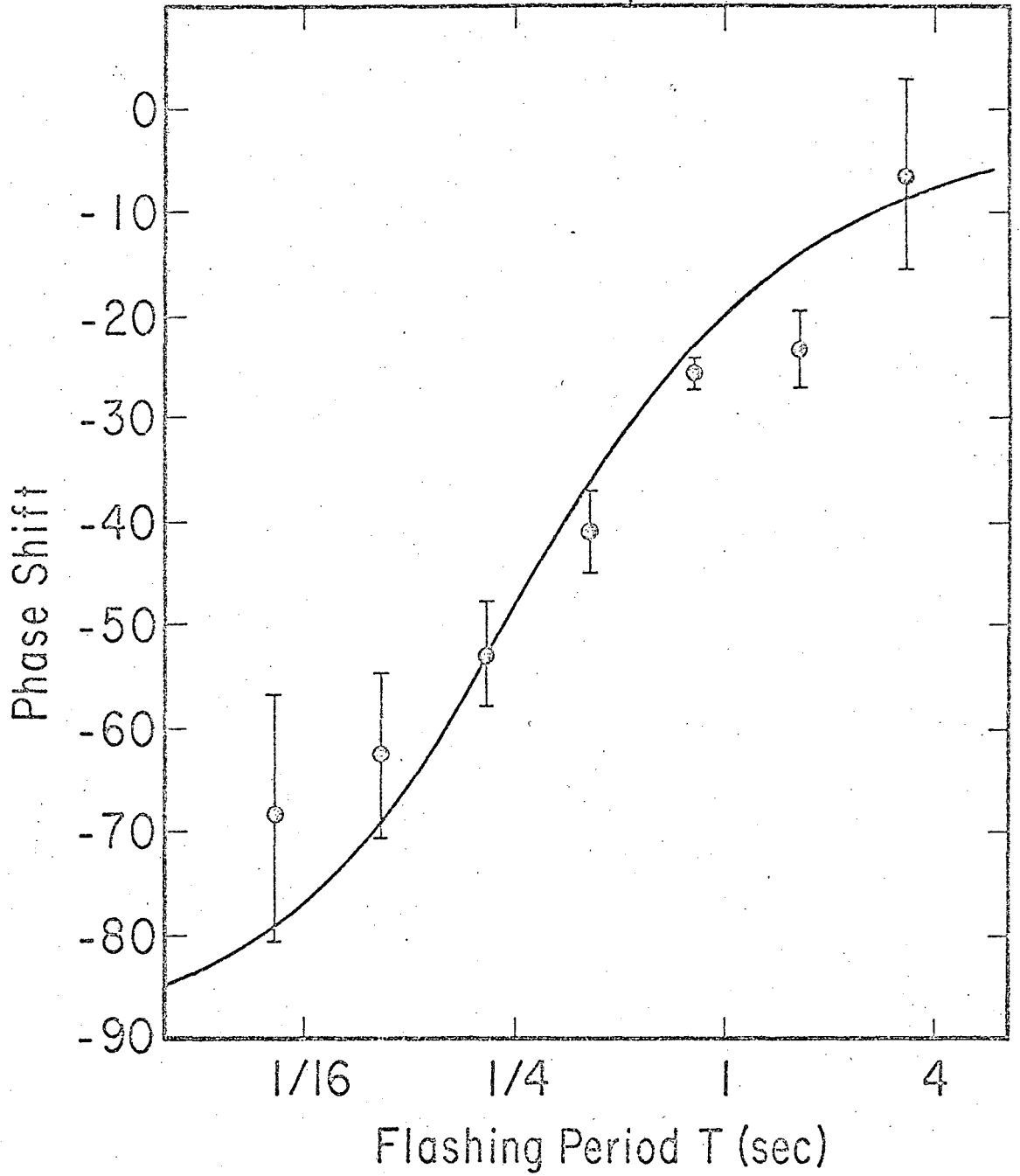
17



XBL 6910-5911

Fig. 18

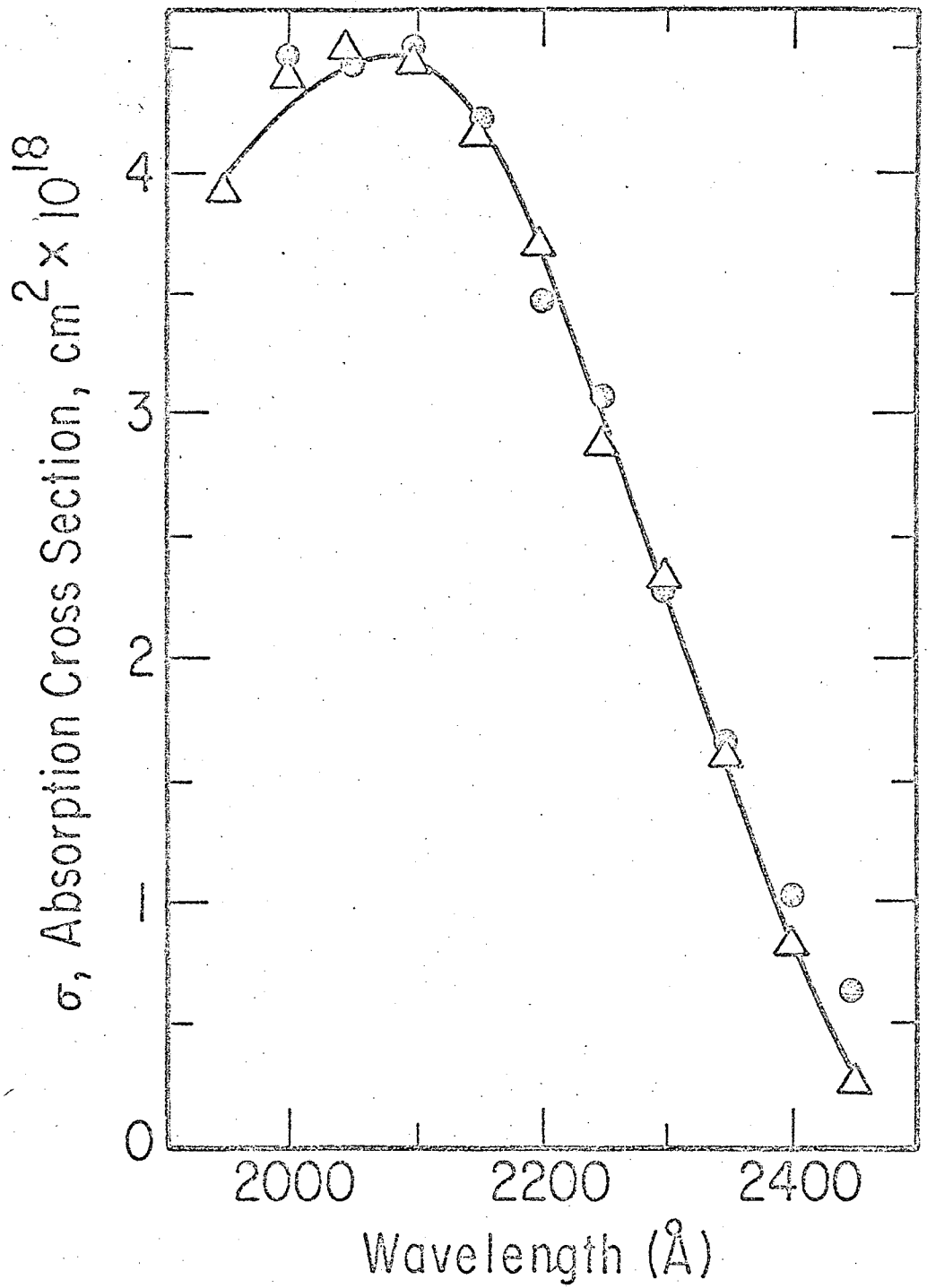
FIG 18 17



XBL 6910-5902

Fig. 19

FIG 19



XBL6910-5896

Fig. 20

LEGAL NOTICE

*This report was prepared as an account of work sponsored by the United States Government. Neither the United States nor the United States Atomic Energy Commission, nor any of their employees, nor any of their contractors, subcontractors, or their employees, makes any warranty, express or implied, or assumes any legal liability or responsibility for the accuracy, completeness or usefulness of any information, apparatus, product or process disclosed, or represents that its use would not infringe privately owned rights.*

TECHNICAL INFORMATION DIVISION  
LAWRENCE BERKELEY LABORATORY  
UNIVERSITY OF CALIFORNIA  
BERKELEY, CALIFORNIA 94720